This article has been accepted for publication in a future issue of this journal, but has not been fully edited. Content may change prior to final publication. Citation information: DOI 10.1109/TSTE.2018.2815502, IEEE Transactions on Sustainable Energy

A Decentralized Renewable Generation Management and Demand Response in Power Distribution Networks

Shahab Bahrami, *Member, IEEE*, M. Hadi Amini, *Graduate Student Member, IEEE*, Miadreza Shafie-khah, *Senior Member, IEEE*, and João P.S. Catalão, *Senior Member, IEEE*

***Abstract*—The stochastic nature of the renewable generators and price-responsive loads, as well as the high computational burden and violation of the generators' and load aggregators' privacy can make the centralized energy market management a big challenge for distribution network operators (DNOs). In this paper, we first formulate the centralized energy trading as a bi-level optimization problem, which is nonconvex and includes the entities' optimal strategy to the price signals. We tackle the uncertainty issues by proposing a probabilistic load model and studying the down-side risk of renewable generation shortage. To address the nonconvexity of the centralized problem, we apply convex relaxation techniques and design proper price signals that guarantee zero relaxation gap. It enables us to address the privacy issue by developing a *decentralized* energy trading algorithm. For the sake of comparison, we use the dual decomposition and proximal Jacobian alternating direction method of multipliers (PJ-ADMM) for the algorithm design. Extensive simulations are performed on different standard test feeders to compare the CPU time of the proposed algorithm with the centralized approach and evaluate its performance in increasing the load aggregators' and generators' profit. Finally, we compare the impact of load and generation uncertainties on the optimality of the results.**

***Keywords*: Price-responsive load, renewable generation, bi-level optimization, decentralized algorithm, uncertainty.**

NOMENCLATURE

- **Abbreviations**

ADMM	Alternating direction method of multipliers.
DNO	Distribution network operator.
ECC	Energy consumption controller.
PAR	Peak-to-average ratio.

- **Variables and Parameters for Generator j**

$\beta_j(h)$	Penalty for generation shortage.
$\rho_j(h)$	Price for active power generation.
$\varrho_j(h)$	Price for reactive power generation.
$\Delta_j(t)$	Uncertainty budget.
$p_j^{\text{con}}(h)$	Conventional unit's output active power.
$p_j^{\text{ren}}(h)$	Offered renewable generation.
$p_j^{\text{avg,ren}}(h)$	Average renewable generation level.
$p_j^{\text{min,ren}}(h)$	Minimum renewable generation level.
$q_j^{\text{con}}(h)$	Conventional unit's output reactive power.

- **Variables and Parameters for Load Aggregator i**

$\mathcal{A}_i^{\text{awake}}(t)$	Set of awake appliances.
$\mathcal{A}_i^{\text{asleep}}(t)$	Set of asleep appliances.
$e_{a,i}(h)$	Power consumption of appliance a.
$\mathcal{H}_{a,i}$	Scheduling horizon of appliance a.
$l_i^{\text{asleep}}(h)$	Total demand of asleep appliances.
$l_i(h)$	Total load demand of all appliances.
ϕ_i	Power factor.

- **Other Variable and Parameters**

h	Index of an arbitrary time slot.
$\mathcal{H}_t$	The time period $\{t, \ldots, H\}$.
t	Index of the current time slot.
$z(h)$	Arbitrary scalar z in time slot h.
$\boldsymbol{z}(t)$	Arbitrary vector $(z(h),\, h \in \mathcal{H}_t)$.
$\delta_b(h)$	Voltage phase angle of bus b.
$v_b(h)$	Voltage magnitude of bus b.
$\Delta v_b(h)$	Voltage drop at bus b.

Manuscript was received on Nov. 20, 2017, revised on Feb. 7, 2018, and accepted on Mar. 7, 2018.

S. Bahrami is graduated from the Department of Electrical and Computer Engineering, the University of British Columbia, Vancouver, BC V6T 1Z4, Canada (email: bahramis@ece.ubc.ca).

M.H. Amini is with the Department of Electrical and Computer Engineering, Carnegie Mellon University, Pittsburgh, PA 15213, USA (email: hadi.amini@ieee.org).

M. Shafie-khah is with C-MAST, University of Beira Interior, Covilhã 6201-001, Portugal (email: miadreza@ubi.pt).

J.P.S. Catalão is with INESC TEC and the Faculty of Engineering of the University of Porto, Porto 4200-465, Portugal, also with C-MAST, University of Beira Interior, Covilhã 6201-001, Portugal, and also with INESC-ID, Instituto Superior Técnico, University of Lisbon, Lisbon 1049-001, Portugal (email:catalao@ubi.pt).

Color versions of one or more of the figures in this paper are available online at http://ieeexplore.ieee.org.

Digital Object Identifier .../TSTE.2018...

I. INTRODUCTION

One goal of the emerging smart grid is to make distribution systems smarter and more secure through integrating a two-way communication infrastructure. The data exchange provides the distribution network operators (DNOs) with sophisticated management techniques to perform complex analyses and automated operations [1]. Meanwhile, different drivers such as distribution organizations have accelerated the applications for smart grid technologies and the integration of renewable generators [2]. The benefits include a more efficient energy usage to reduce the load aggregators' payment, a lower operation cost for the generators, and a higher flexibility for

1949-3029 (c) 2018 IEEE. Personal use is permitted, but republication/redistribution requires IEEE permission. See http://www.ieee.org/publications_standards/publications/rights/index.html for more information.

This article has been accepted for publication in a future issue of this journal, but has not been fully edited. Content may change prior to final publication. Citation information: DOI 10.1109/TSTE.2018.2815502, IEEE Transactions on Sustainable Energy

the DNO to improve the system's technical operation; thereby reaching a triple-win result [3], [4].

The power system analysis and control is a challenging task for the DNO. First, the uncertainties in the load demand and renewable generation can cause unpredicted problems, such as the voltage drop/rise. The second challenge is the violation of the entities' privacy, e.g., revealing the load aggregators' demand information and generators' cost parameters to the DNO. Third, the system analysis can be computationally difficult, especially when the number of decision variables increases with the participation of price-responsive load aggregators and renewable generators in the energy market.

There have been some efforts in the literature to tackle the above-mentioned challenges. We divide the related works into three main threads. The first thread is concerned with decentralized energy management programs for a market with multiple suppliers and multiple users. Mechanisms such as the multi-level game [5], Stackelberg game [6], dual decomposition [7], and hierarchical bidding [8], [9] have been used. However, these approaches did not consider the constraints imposed by the topology and operation of the distribution network. The second thread is concerned with including the power flow equations in the decentralized energy management procedure. To achieve this goal, different techniques such as convex relaxation [10]–[12], quadratic programming [13], alternating direction method of multipliers (ADMM) [14]–[16], and Lagrange relaxation method [17]–[19] have been used. These studies, however, did not consider the uncertainties of the renewable generators and load demand. Furthermore, they mainly focused on off-line algorithms, which are applicable to day-ahead markets. The third thread concerned with the online operation of distribution systems using different mechanisms such as real-time closed-loop control [20], differential evolution optimization [21], [22], stochastic programming [23], online gradient method [24], projected gradient descent [25], and online mirror descent [26]. These works, however, did not mention how to consider the uncertainty of the load demand for different types of users.

A. Goals and Contributions

Although there exist several studies on the energy market with multiple load aggregators and generators (e.g., [5]–[26]), the impact of uncertainties in the generation and load demand on the online decision making of the entities has not been studied comprehensively yet. In this paper, we focus on designing a decentralized algorithm for an energy trading market with renewable energy generators and price-responsive load aggregators. In each time slot (e.g., every 15 minutes), the load aggregators and generators jointly maximize their own profit, while considering the uncertainty in the future demand and renewable generation. The entities' privacy is protected, as the generators and load aggregators solve their own profit maximizing problem using the locally available information.

The load management decision (e.g., load shifting, load curtailment) of a load aggregator in the *current* time slot affects its demand during the *upcoming* time slots. Meanwhile, the generators must match their generation levels with the changes

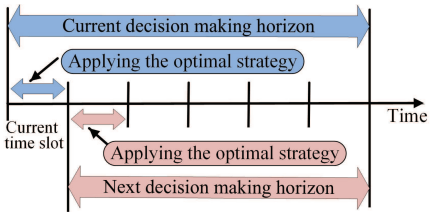

Figure 1. The receding horizon control for energy trading.

in the load demands. It implies that for decision making in the current time slot, the generation-load balance during the current and upcoming time slots should be considered. Our goal is to propose a *receding horizon* energy trading algorithm for the load aggregators and generators. As Fig. 1 depicts, the decision making horizon of the entities starts from the current time until the end of the trading horizon. But, the entities only apply the optimal decision for the current time. This process is repeated for the next time slots. The main challenges that we address are to tackle the uncertainty in the load demand and renewable generation, as well as to determine the appropriate control signals exchanged between the DNO, generators, and load aggregators that enforce the proposed decentralized algorithm to converge to the solution of the DNO's *centralized* problem with the objective of maximizing the social welfare. This paper is an extension of our previous work [27] by considering the renewable generation and load demand uncertainties, as well as proposing an autonomous energy trading in real-time energy markets. In particular, we aim to answer two key questions:

Q.1 How do the entities determine their strategy in the *current* time slot with the locally available information?

Q.2 How do the entities address the lack of information about the demand and generation in the *future* time slots?

The main contributions of this paper are as follows:

- *Problem Formulation:* We formulate the DNO's centralized approach as a bi-level optimization problem. In the outer level, the social welfare is maximized by considering the network's physical constraints using the *linearized ac power flow* and the impacts of the renewable generation shortage on the bus voltages. The inner level includes the optimal responses of the load aggregators and generators to the price signals. To address the non-convexity of the problem, we use convex relaxation technique incorporated with a price signal design procedure such that the relaxation gap becomes zero.
- *Addressing the Uncertainty Issues:* To address the uncertainty in the demand of the load aggregators, we propose a probabilistic load estimation for the electric appliances of the consumers. It enables each load aggregator to take into account the impacts of the future load profiles on the current scheduling decisions of the appliances. We also consider an adaptive uncertainty set for the renewable generators to study the down-side risk of renewable generation shortage. It enables a generator to wisely offer its renewable generation profile such that a high penalty for power shortage is avoided. The DNO can also secure the grid against a high voltage drop.

1949-3029 (c) 2018 IEEE. Personal use is permitted, but republication/redistribution requires IEEE permission. See http://www.ieee.org/publications_standards/publications/rights/index.html for more information.

This article has been accepted for publication in a future issue of this journal, but has not been fully edited. Content may change prior to final publication. Citation information: DOI 10.1109/TSTE.2018.2815502, IEEE Transactions on Sustainable Energy

- *Distributed Algorithm Design:* We first use the dual decomposition technique [28] to develop a decentralized algorithm that protects the privacy of the entities and addresses the computational complexity of the centralized problem. The proposed algorithm provably converges to the solution of the centralized problem. This approach has been used in [17], [18]. Next, we modify our algorithm to a proximal Jacobian ADMMM (PJ-ADMM)-based algorithm [29, Algorithm 4] in order to improve the convergence speed. It is preferable to the proposed variable splitting ADMM-based algorithm in [14]–[16], as introducing the splitting variables substantially increases the number of variables and constraints in the problem.
- *Performance Evaluation:* Simulations are performed on the IEEE 123-bus test feeder with 5 generators and 118 load aggregators. When compared with the benchmark of not performing load management and not using renewable generation, the proposed decentralized algorithm benefits the load aggregators and generators by increasing their profit by 23.34% and 15.2% on average, respectively. It also helps the generators to reduce the peak-to-average ratio (PAR) by 16.9%. Our algorithm converges to the solution of the centralized problem with a significantly lower execution time and a smaller number of iterations. The PJ-ADMM-based algorithm converges faster compared to the dual decomposition-based algorithm. When compared with the full ac power flow model, the optimal objective value with the linearized ac power flow model is slightly smaller (by 1.2% to 2.9%) due to power losses impact. Our approach returns a near-optimal load scheduling, as the difference between the scheduled load profiles with and without uncertainty is only 3.84%.

The rest of this paper is organized as follows. Section II introduces the system model. In Section III, the DNO's centralized problem is formulated. In Section IV, a decentralized algorithm is proposed to solve the DNO's problem. Section V provides the simulation results, followed by Section VI that concludes the paper.

II. System Model

As shown in Fig. 2, consider a distribution network with a set $\mathcal{I}$ of load aggregators and a set $\mathcal{G}$ of generators. Each load aggregator is responsible for managing the load demand of its electricity consumers (e.g., residential households, commercial sectors). Each generator sells electricity to the grid. The load aggregators and generators use a two-way communication infrastructure to exchange necessary information with the DNO, which is a neutral entity responsible for monitoring the power flow in the network. The trading horizon is denoted by $\mathcal{H} \triangleq \{1, \ldots, H\}$, where H is the number of time slots with an equal length (e.g., each time slot is 15 minutes). For simplicity in the problem formulation, we assume that each bus has *exactly* one load aggregator or one generator. It enables us to denote the set of buses by $|\mathcal{I} \cup \mathcal{G}|$ and uniquely denote a load aggregator or a generator by its bus index. Let $\mathcal{L}$ denote the set of branches in the network.

To avoid an abuse of notations, we use index h for a time slot in general and use index t specifically for the *current* time slot. At the beginning of the current time slot t, the entities observe the updated information and optimize their demand/supply during the period $\mathcal{H}_t = \{t, \ldots, H\} \subseteq \mathcal{H}$, but they apply only the decision for the current time slot t. The scheduling is performed with uncertainty about the demands and (renewable) generation in the future time slots $h > t$. In the following subsections, we discuss the models of generators and load aggregators.

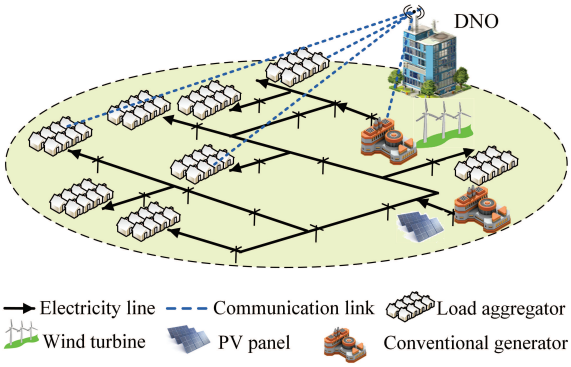

Figure 2. A distribution network consisting of a DNO, several load aggregators, and several generators with renewable and conventional power plants.

A. Generator's Model

In this subsection, we model the conventional and renewable units of a generator, and formulate a generator's local problem.

1) Conventional Plant Model: In the current time slot t, generator $j \in \mathcal{G}$ with a conventional unit offers the active power profile $\boldsymbol{p}_j^{\text{con}}(t) = (p_j^{\text{con}}(h), h \in \mathcal{H}_t)$. The generation cost function of the conventional unit of generator j in time slot h can be modeled by a continuous increasing convex function of the output power $p_j^{\text{con}}(h)$, e.g., the following class of quadratic functions has been commonly used:

$$C_j^{\text{con}}(p_j^{\text{con}}(h)) = a_{j2}\left(p_j^{\text{con}}(h)\right)^2 + a_{j1}p_j^{\text{con}}(h) + a_{j0}, \quad (1)$$

where a_{j0}, a_{j1}, and a_{j2} are positive coefficients. The output active power of a conventional unit is bounded. That is

$$p_j^{\text{min,con}} \le p_j^{\text{con}}(h) \le p_j^{\text{max,con}}, \quad h \in \mathcal{H}_t. \quad (2)$$

A conventional generation unit can inject/absorb reactive power, which can be represented by operating with lagging or leading power factors. Let $\boldsymbol{q}_j^{\text{con}}(t) = (q_j^{\text{con}}(h), h \in \mathcal{H}_t)$ denote the injected reactive power profile of generator j. The generator's loading capability determines the restriction on the injected reactive power, which is limited by the the generator's armature current limit, the filed current limit, and the under-excitation limit. For $h \in \mathcal{H}_t$, the constraints for a typical capability curve of a generator are as follows [30, Ch. 5.4]:

$$\left(p_j^{\text{con}}(h)\right)^2 + \left(q_j^{\text{con}}(h)\right)^2 \le \left(p_j^{\text{max,con}}\right)^2, \quad (3a)$$

$$\left(p_j^{\text{con}}(h)\right)^2 + \left(q_j^{\text{con}}(h) - q_j^{\text{field}}\right)^2 \le \left(q_j^{\text{max,con}} - q_j^{\text{field}}\right)^2, \quad (3b)$$

$$\left(p_j^{\text{con}}(h)\right)^2 + \left(q_j^{\text{con}}(h) - q_j^{\text{end}}\right)^2 \le \left(q_j^{\text{end}} - q_j^{\text{min,con}}\right)^2, \quad (3c)$$

where $q_j^{\text{field}} > 0$ and $q_j^{\text{end}} < 0$ are constants depending on the specifications of the generator. $q_j^{\text{min,con}}$ and $q_j^{\text{max,con}}$ are the

1949-3029 (c) 2018 IEEE. Personal use is permitted, but republication/redistribution requires IEEE permission. See http://www.ieee.org/publications_standards/publications/rights/index.html for more information.

This article has been accepted for publication in a future issue of this journal, but has not been fully edited. Content may change prior to final publication. Citation information: DOI 10.1109/TSTE.2018.2815502, IEEE Transactions on Sustainable Energy

lower and upper bounds for the reactive power of generator j, respectively. The feasible space defined by (2) and (3) is closed and convex. For the reactive power generation $q_j^{\text{con}}(h)$, we can determine a unique upper bound for $p_j^{\text{con}}(h)$ as $\mathcal{F}(q_j^{\text{con}}(h))$, where $\mathcal{F}(\cdot)$ is a strongly concave function.

2) Renewable Plant Model: In the current time slot t, generator j with a renewable unit offers an active power profile $\boldsymbol{p}_j^{\text{ren}}(t) = (p_j^{\text{ren}}(h),\, h \in \mathcal{H}_t)$. We make the following assumption regarding the output reactive power of the renewable units:

Assumption 1: The renewable plant of generator $j \in \mathcal{G}$ is operated at unity power factor.

Renewable units (e.g., wind turbines) are generally equipped with power electronic converters, and thus they can control their output reactive power. One can consider the P-Q characteristics of the converters [31] to obtain the operational constraints similar to (3) for the renewable units. In our system model, the conventional unit of generator j can control its output reactive power. Hence without loss of generality, we can make Assumption 2 and allow the conventional unit performs the reactive power compensation in bus j.

An accurate prediction of the renewable generation is a challenge for a generator. The deviation of the actual renewable generation from the predicted generation can cause voltage rise/drop in the grid. The generator may simply choose to curtail the renewable generation surplus at almost no cost, and thus the voltage rise can be avoided. In the case of supply shortage, however, the network experiences voltage drop, and the DNO must operate backup generators to alleviate the generation shortage. The DNO charges generator j by the prices $\beta_j(h),\, h \in \mathcal{H}_t$ (\$/MWh) that depend on the cost of alleviating the generation shortage. This penalty can motivate generator j to avoid overestimation of its renewable generation. Generator j can use the historical data record to forecast the average generation level $p_j^{\text{avg,ren}}(h)$, as well as a symmetric uncertainty bound $[p_j^{\text{min,ren}}(h), p_j^{\text{max,ren}}(h)]$ around the average value for its *actual* renewable generation in time slots $h \in \mathcal{H}_t$. A worst-case model is particularly attractive when the probability distribution of the renewable generation is unavailable to the generator or the DNO. The worst-case generation shortage of generator j is equal to $p_j^{\text{ren}}(h) - p_j^{\text{min,ren}}(h) - (\mathcal{F}(q_j^{\text{con}}(h)) - p_j^{\text{con}}(h))$, where $p_j^{\text{ren}}(h) - p_j^{\text{min,ren}}(h)$ is the worst-case renewable generation shortage and $\mathcal{F}(q_j^{\text{con}}(h)) - p_j^{\text{con}}(h)$ is the reserved capacity for increasing the conventional generation from $p_j^{\text{con}}(h)$ to the upper bound $\mathcal{F}(q_j^{\text{con}}(h))$.

The *down-side risk* associated with the generation shortage of generator j in time slot h can be defined as the worst-case cost of generation shortage. Generator j considers $\Gamma_j(\boldsymbol{p}_j^{\text{ren}}(t), \boldsymbol{q}_j^{\text{con}}(t))$ as the the down-side risk of generation shortage during the upcoming time period $\mathcal{H}_t$ as follows:

$$\Gamma_j(\boldsymbol{p}_j^{\text{ren}}(t), \boldsymbol{q}_j^{\text{con}}(t)) = \sum_{h\in\mathcal{H}_t} \beta_j(h) \Big(p_j^{\text{ren}}(h) - p_j^{\text{min,ren}}(h) - \big(\mathcal{F}(q_j^{\text{con}}(h)) - p_j^{\text{con}}(h)\big)\Big). \quad (4)$$

Note that the down-side risk (4) is the maximum cost of generation shortage. Hence, our problem is to minimize the maximum cost of generation shortage (similar to the min-max problem in a robust optimization technique), and the solution to the maximum cost of generation shortage is given in (4).

For decision making in the current time slot, minimizing (4) will guarantee a low risk of large penalty for the generator. However, for large values of $\beta_j(h)$, minimizing (4) leads to offering $p_j^{\text{ren}}(h)$ around $p_j^{\text{min,ren}}(h)$, which is very conservative and possibly inefficient. Inspired by the work in [32], we consider the following adaptive ellipsoidal uncertainty space for the generation profile $\boldsymbol{p}_j^{\text{ren}}(t)$ in the current time slot t:

$$\mathcal{P}_j^{\text{ren}}(t) = \Bigg\{ \boldsymbol{p}_j^{\text{ren}}(t) \;\Big|\; p_j^{\text{ren}}(h) \in \Big[p_j^{\text{min,ren}}(h), p_j^{\text{max,ren}}(h)\Big],\; \sum_{h\in\mathcal{H}_t} \left[\frac{p_j^{\text{avg,ren}}(h) - p_j^{\text{ren}}(h)}{p_j^{\text{avg,ren}}(h) - p_j^{\text{min,ren}}(h)}\right]^2 \le \Delta_j(t) \Bigg\}, \quad (5)$$

where $0 \le \Delta_j(t) \le |\mathcal{H}_t|$ is the uncertainty budget for generator j in the current time slot t. If $\Delta_j(t) = 0$, then the space defined in (5) is a singleton, corresponding to the scenario $p_j^{\text{ren}}(h) = p_j^{\text{avg,ren}}(h),\, h \in \mathcal{H}_t$. As $\Delta_j(t)$ increases, the size of the uncertainty set enlarges. The space includes all possible scenarios when $\Delta_j(t) = |\mathcal{H}_t|$. In [32], $\Delta_j(t) \approx \sqrt{|\mathcal{H}_t|}$ is suggested to provide an acceptable uncertainty set. For $\Delta_j(t) = 0$, generator j offers the desirable generation profile $p_j^{\text{avg,ren}}(h),\, h \in \mathcal{H}_t$. Increasing the value of $\Delta_j(t)$ causes the generator to offer $p_j^{\text{ren}}(h)$ less than $p_j^{\text{avg,ren}}(h),\, h \in \mathcal{H}_t$. Although the down-side risk in (4) becomes smaller, but the revenue from selling renewable generation would be small too, which can cause dissatisfaction for the generator. We consider a discomfort cost function $D_j(\boldsymbol{p}_j^{\text{ren}}(t))$ to model the dissatisfaction of generator j by deviating its renewable generation profile from the desirable profile $p_j^{\text{avg,ren}}(h),\, h \in \mathcal{H}_t$. That is,

$$D_j\left(\boldsymbol{p}_j^{\text{ren}}(t)\right) = d_j \sum_{h\in\mathcal{H}_t} \left(p_j^{\text{avg,ren}}(h) - p_j^{\text{ren}}(h)\right)^2. \quad (6)$$

The cost in (6) is based on the Euclidean distance between the profiles of offered and desirable renewable productions. Parameter d_j is a weight coefficient in \$/(MWh)^2 that converts the discomfort of generator j to the monetary units.

3) Local Optimization Problem: In the current time slot t, generator j determines the decision variable $\boldsymbol{x}_j(t) = (\boldsymbol{p}_j^{\text{con}}(t), \boldsymbol{q}_j^{\text{con}}(t), \boldsymbol{p}_j^{\text{ren}}(t))$. The objective of generator j is to maximize its profit $\pi_j^{\text{gen}}(\boldsymbol{x}_j(t))$, which is the revenue from selling active and reactive powers with prices $\boldsymbol{\rho}_j(t) = (\rho_j(h),\, h \in \mathcal{H}_t)$ and $\boldsymbol{\varrho}_j(t) = (\varrho_j(h),\, h \in \mathcal{H}_t)$ minus the cost of conventional generation and the cost associated with the renewable generation shortage with penalties $\boldsymbol{\beta}_j(t) = (\beta_j(h),\, h \in \mathcal{H}_{t+1})$. That is,

$$\pi_j^{\text{gen}}(\boldsymbol{x}_j(t)) = \sum_{h\in\mathcal{H}_t} \Big(\left(p_j^{\text{con}}(h) + p_j^{\text{ren}}(h)\right)\rho_j(h) + q_j(h)\varrho_j(h) - C_j^{\text{con}}\left(p_j^{\text{con}}(h)\right)\Big) - D_j(\boldsymbol{p}_j^{\text{ren}}(t)) - \Gamma_j\left(\boldsymbol{p}_j^{\text{ren}}(t), \boldsymbol{q}_j^{\text{con}}(t)\right). \quad (7)$$

The problem for generator $j \in \mathcal{G}$ in the current time slot t is

$$\underset{\boldsymbol{x}_j(t)}{\text{maximize}}\; \pi_j^{\text{gen}}(\boldsymbol{x}_j(t))$$
$$\text{subject to constraints (2)}-\text{(3)}, \quad (8a)$$
$$\boldsymbol{p}_j^{\text{ren}}(t) \in \mathcal{P}_j^{\text{ren}}(t). \quad (8b)$$

1949-3029 (c) 2018 IEEE. Personal use is permitted, but republication/redistribution requires IEEE permission. See http://www.ieee.org/publications_standards/publications/rights/index.html for more information.

This article has been accepted for publication in a future issue of this journal, but has not been fully edited. Content may change prior to final publication. Citation information: DOI 10.1109/TSTE.2018.2815502, IEEE Transactions on Sustainable Energy

Functions $C_j^{\text{con}}(p_j^{\text{con}}(h))$ and $D_j(\boldsymbol{p}_j^{\text{ren}}(t))$ are strongly convex. Furthermore, $\Gamma_j(\boldsymbol{p}_j^{\text{ren}}(t), \boldsymbol{q}_j^{\text{con}}(t))$ in (4) includes the strongly concave function $\mathcal{F}(q_j^{\text{con}}(h))$. Hence, the objective function (7) is strongly concave. The feasible space $\mathcal{X}_j(t)$ defined by (8a) and (8b) is convex and compact. Therefore, if problem (8) is feasible, then it has a unique optimal solution $\boldsymbol{x}_j^*(t)$.

We consider the optimal control decision of the current time slot t for generator j given vector $(\boldsymbol{\rho}_j(t), \boldsymbol{\varrho}_j(t), \boldsymbol{\beta}_j(t))$ as

$$\mathcal{B}_j\left(\boldsymbol{\rho}_j(t), \boldsymbol{\varrho}_j(t), \boldsymbol{\beta}_j(t)\right) := \underset{\boldsymbol{x}_j(t)\in\mathcal{X}_j(t)}{\operatorname{argmax}} \quad \pi_j^{\text{gen}}(\boldsymbol{x}_j(t)). \tag{9}$$

B. Load Aggregator's Model

In this subsection, we discuss the model for the load aggregators. As Fig. 3 shows, a load aggregator may serve multiple consumers. A consumer is equipped with an energy consumption controller (ECC), which is responsible for monitoring the consumers' appliances as well as providing the load aggregator with necessary information through the communication network on behalf of the consumer. In the following, we discuss the consumers' appliances model.

1) Consumers' Appliances Model: In the current time slot t, an electric appliance is either *asleep* or *awake*. Let $\mathcal{A}_i^{\text{asleep}}(t)$ and $\mathcal{A}_i^{\text{awake}}(t)$ denote the sets of asleep and awake appliances of all consumers in the current time slot t, respectively. An awake appliance $a \in \mathcal{A}_i^{\text{awake}}(t)$ is available to be scheduled for operation, i.e., the load aggregator schedules the power consumption profile $\boldsymbol{e}_{a,i}(t) = (e_{a,i}(h),\, h \in \mathcal{H}_t)$.

The ECC provides the load aggregator i with the scheduling horizon, utility function, and type of an awake appliance $a \in \mathcal{A}_i^{\text{awake}}(t)$ of its consumers. The scheduling horizon $\mathcal{H}_{a,i} \subseteq \mathcal{H}_t$ defines the time interval, in which the appliance should operate. The utility function $U_{a,i}(\boldsymbol{e}_{a,i}(t))$ is used to model the satisfaction of the customer in monetary units from using the appliance. We make the following assumption [33, Ch. 1]:

Assumption 2: For appliance a, the utility $U_{a,i}(\boldsymbol{e}_{a,i}(t))$ is an increasing concave function of the consumption profile $\boldsymbol{e}_{a,i}(t)$.

The increasing concavity of $U_{a,i}(\boldsymbol{e}_{a,i}(t))$ implies that the utility of using appliance a increases by $\boldsymbol{e}_{a,i}(t)$, but the rate of change decreases with $\boldsymbol{e}_{a,i}(t)$. The type of appliance depends on its specifications and the customer's preferences. Inspired by the work in [34], we consider three types of appliances:

a) Type 1 Appliances: The appliance a of type 1 should be operated within the scheduling horizon $\mathcal{H}_{a,i}$ and turned off during other time slots, e.g., electric vehicle (EV). Let $\mathcal{A}_i^1(t) \subseteq \mathcal{A}_i^{\text{awake}}(t)$ denote the set of appliances of type 1 that are awake in the current time slot t. For $a \in \mathcal{A}_i^1(t)$, we have

$$e_{a,i}(h) = 0, \qquad h \notin \mathcal{H}_{a,i}, \tag{10a}$$
$$e_{a,i}^{\min}(h) \le e_{a,i}(h) \le e_{a,i}^{\max}(h), \qquad h \in \mathcal{H}_{a,i}, \tag{10b}$$
$$E_{a,i}^{\min} \le \sum_{h\in\mathcal{H}_{a,i}} e_{a,i}(h) \le E_{a,i}^{\max}. \tag{10c}$$

The utility obtained from using a type 1 appliance depends on the total power consumption. The utility can be expressed as $U_{a,i}(\boldsymbol{e}_{a,i}(t)) = U_{a,i}\left(\sum_{h\in\mathcal{H}_{a,i}} e_{a,i}(h)\right)$, e.g., $\kappa_{a,i}\, u\left(\sum_{h\in\mathcal{H}_{a,i}} e_{a,i}(h) - E_{a,i}^{\min}\right)$ with an increasing concave function $u(\cdot)$ and nonnegative constant $\kappa_{a,i}$.

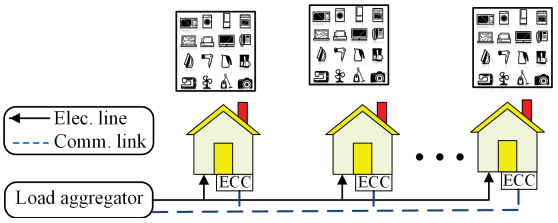

Figure 3. A load aggregator is connected to the ECC of each consumer via a two-way communication network.

b) Type 2 Appliances: The appliances of type 2 can be operated in time slots out of the scheduling horizon, but the customer attains a relatively lower utility, e.g., TV and PC. Let $\mathcal{A}_i^2(t) \subseteq \mathcal{A}_i^{\text{awake}}(t)$ denote the set of appliances of type 2 that are awake in time slot t. For $a \in \mathcal{A}_i^2(t)$, we have

$$e_{a,i}(h) \ge 0, \qquad h \notin \mathcal{H}_{a,i}, \tag{11a}$$
$$e_{a,i}^{\min}(h) \le e_{a,i}(h) \le e_{a,i}^{\max}(h), \qquad h \in \mathcal{H}_{a,i}, \tag{11b}$$
$$E_{a,i}^{\min} \le \sum_{h\in\mathcal{H}_{a,i}} e_{a,i}(h) \le E_{a,i}^{\max}. \tag{11c}$$

The utility function of type 2 appliances depends on both the amount of power consumption and the time of consuming the power, i.e., the customer would gain different benefits from consuming the same amount of power at different times, e.g., watching the favorite TV program. We have $U_{a,i}(\boldsymbol{e}_{a,i}(t)) = \sum_{h\in\mathcal{H}_t} U_{a,i}(e_{a,i}(h), h)$. As an example, utility function $U_{a,i}(\boldsymbol{e}_{a,i}) = \sum_{h\in\mathcal{H}_{a,i}} \kappa_{a,i}(h)\, u\big(e_{a,i}(h) - e_{a,i}^{\min}\big) + \sum_{k\notin\mathcal{H}_{a,i}} \kappa'_{a,i}(h)\, u\big(e_{a,i}(h)\big)$ with an increasing concave function $u(\cdot)$ and *time dependent* nonnegative coefficients $\kappa_{a,i}(h)$ and $\kappa'_{a,i}(h)$, $\kappa'_{a,i}(h) \ll \kappa_{a,i}(h)$ is a viable candidate.

c) Type 3 Appliances: The appliances of type 3 can be operated out of the scheduling horizon without any constraint on their total power consumption, such as lighting and refrigerator. Let $\mathcal{A}_i^3(t) \subseteq \mathcal{A}_i^{\text{awake}}(t)$ denote the set of currently awake appliances of type 3. For $a \in \mathcal{A}_i^3(t)$, we have

$$e_{a,i}(h) \ge 0, \qquad h \notin \mathcal{H}_{a,i}, \tag{12a}$$
$$e_{a,i}^{\min}(h) \le e_{a,i}(h) \le e_{a,i}^{\max}(h), \qquad h \in \mathcal{H}_{a,i}. \tag{12b}$$

The utility $U_{a,i}(\boldsymbol{e}_{a,i})$ attained by the customer from using the appliances of type 3 depends on the amount of power consumption $e_{a,i}(t)$ within the scheduling horizon $\mathcal{H}_{a,i}$, but not the time of consumption. The customer attains a relatively lower utility out of interval $\mathcal{H}_{a,i}$. For example, function $U_{a,i}(\boldsymbol{e}_{a,i}) = \sum_{h\in\mathcal{H}_{a,i}} \kappa_{a,i}\, u\big(e_{a,i}(h) - e_{a,i}^{\min}\big) + \sum_{h\notin\mathcal{H}_{a,i}} \kappa'_{a,i}\, u\big(e_{a,i}(h)\big)$ with an increasing concave function $u(\cdot)$ and nonnegative *constants* $\kappa_{a,i}$ and $\kappa'_{a,i}$, $\kappa'_{a,i} \ll \kappa_{a,i}$ is a viable candidate. The total utility of load aggregator i in time slot t with decision $\boldsymbol{x}_i(t) = (\boldsymbol{e}_{a,i}(t),\, a \in \mathcal{A}_i^{\text{awake}}(t))$ is

$$U_i(\boldsymbol{x}_i(t)) = \sum_{a\in\mathcal{A}_i^{\text{awake}}(t)} U_{a,i}(\boldsymbol{e}_{a,i}(t)), \quad i \in \mathcal{I}. \tag{13}$$

2) Load Estimation: The scheduling of the awake appliances depends not only on the current demand, but also on the demand in future time slots. For example, if the future demand is predicted to be high, then the currently awake appliances

1949-3029 (c) 2018 IEEE. Personal use is permitted, but republication/redistribution requires IEEE permission. See http://www.ieee.org/publications_standards/publications/rights/index.html for more information.

This article has been accepted for publication in a future issue of this journal, but has not been fully edited. Content may change prior to final publication. Citation information: DOI 10.1109/TSTE.2018.2815502, IEEE Transactions on Sustainable Energy

may be scheduled to operate at the current time slot.

The actual wake-up times of the appliances are not available to the load aggregator in advance. To address this lack of information, load aggregator i can collect the sleep-awake historical data record of each appliance and estimate the probability $p_{a,i}(h)$ that each appliance $a \in \mathcal{A}_i$ becomes awake at each time slot $h \in \mathcal{H}$. In practice, it may not be possible for the load aggregator to reliably estimate the appliances availability at the consumers' appliance level. As Fig. 3 shows, for practical implementation, the ECCs collect the appliances' sleep-awake historical data record and provide the corresponding load aggregator with this information via the communication network [35], [36]. In appendix A, we show the *conditional* probability $p_{a,i}(h \,|\, t)$ that the appliance becomes awake in an upcoming time slot $h > t$, given that it has not become awake until the current time slot, t, is

$$p_{a,i}(h \,|\, t) = \frac{p_{a,i}(h)}{1 - \sum_{h'=1}^{t} p_{a,i}(h')}. \tag{14}$$

A load aggregator has limited information about the scheduling horizon, users' utility functions, and type of the appliances ahead of time. Predicting the controllability of an appliance is a challenge with the lack of information about the flexibility of a currently sleeping appliance. Thus, we consider the *worst-case scenario* for the load demand in future time slot, where the appliances that become awake in time slots $h > t$ should be operated once they become awake without any control on their power and energy consumption. Mathematically, the appliances are of type 1 and operate with the nominal rating power $e_{a,i}^{\text{nom}}$ and nominal energy demand $E_{a,i}^{\text{nom}}$, i.e., $e_{a,i}^{\min}(h) = e_{a,i}^{\max}(h) = e_{a,i}^{\text{nom}}$ and $E_{a,i}^{\min} = E_{a,i}^{\max} = E_{a,i}^{\text{nom}}$.

The payment of the load aggregator in the worst-case scenario is an upper-bound for its actual payment. Minimizing the worst-case payment implies reducing the *risk* of high payment. The expected electric demand $l_i^{\text{asleep}}(h)$ of the asleep appliances in an upcoming time slot $h > t$ is obtained as

$$l_i^{\text{asleep}}(h) = \sum_{a \in \mathcal{A}_i^{\text{asleep}}(t)} \sum_{h'=\max\{t+1,\, h-T_a+1\}}^{h} e_{a,i}^{\text{nom}}(h)\, p_{a,i}(h' \,|\, t), \tag{15}$$

where parameter $T_a = E_{a,i}^{\text{nom}} / e_{a,i}^{\text{nom}} \geq 1$ is the operation duration of the appliance $a \in \mathcal{A}_i^{\text{asleep}}(t)$ that becomes awake with the nominal specifications in the time slot $h > t$. The summation in the brackets is equal to the probability that the currently sleeping appliance a is *operating* in time slot $h > t$.

Let $\boldsymbol{l}_i(t) = (l_i(h),\, h \in \mathcal{H}_t)$ denote the profile of total *active power* consumption of load aggregator i during the time interval $\mathcal{H}_t$. We have

$$l_i(h) = l_i^{\text{asleep}}(h) + \sum_{a \in \mathcal{A}_i^{\text{awake}}(t)} e_{a,i}(h), \qquad h \in \mathcal{H}_t. \tag{16}$$

To model the *reactive power* consumption for load aggregator i, we consider a constant power factor ϕ_i. The reactive power for load aggregator i in time h is $l_i(h)\text{sgn}(\phi_i)\sqrt{(1-\phi_i^2)/\phi_i^2}$, where $\text{sgn}(\cdot)$ is the sign function.

3) Local Optimization Problem: Constraints (10a)−(16) define the feasible space $\mathcal{X}_i(t)$ for decision vector $\boldsymbol{x}_i(t)$ of load aggregator i in the current time slot t. Load aggregator i aims to maximize the profit $\pi_i^{\text{agg}}(\boldsymbol{x}_i(t))$, which includes the total utility in (13) minus the payment to the DNO during period $\mathcal{H}_t$. The DNO provides load aggregator i with price $\rho_i(h)$ for active power in each time slot h. We assume that load aggregators do not pay for the reactive power. We have

$$\pi_i^{\text{agg}}(\boldsymbol{x}_i(t)) = U_i(\boldsymbol{x}_i(t)) - \sum_{h \in \mathcal{H}_t} l_i(h)\, \rho_i(h), \quad i \in \mathcal{I}. \tag{17}$$

Load aggregator i solves the following optimization problem in time slot t to determine its decision vector $\boldsymbol{e}_i(t)$:

$$\underset{\boldsymbol{x}_i(t)}{\text{maximize}} \;\; \pi_i^{\text{agg}}(\boldsymbol{x}_i(t)) \tag{18a}$$

$$\text{subject to} \;\; \boldsymbol{x}_i(t) \in \mathcal{X}_i(t). \tag{18b}$$

Because (17) is strongly concave and the feasible space $\mathcal{X}_i(t)$ is convex and compact, a *unique* solution $\boldsymbol{x}_i^*(t)$ to problem (18) exists if this problem is feasible. We consider the *optimal* decision in the current time slot t for load aggregator i given the market price vector $\boldsymbol{\rho}_i(t) = (\rho_i(h),\, h \in \mathcal{H}_t)$ as

$$\boldsymbol{x}_i^*(t) = \mathcal{B}_i(\boldsymbol{\rho}_j(t)) := \underset{\boldsymbol{x}_i(t) \in \mathcal{X}_i(t)}{\text{argmax}} \; \pi_i^{\text{agg}}(\boldsymbol{x}_i(t)). \tag{19}$$

III. DNO's Risk-Aware Social-welfare Problem

We consider the objective of maximizing the social welfare for the DNO. Consider the grid-wide decision variable $\boldsymbol{x}(t) = (\boldsymbol{x}_b(t),\, b \in \mathcal{G} \cup \mathcal{I})$. The DNO's objective function is

$$f^{\text{DNO}}(\boldsymbol{x}(t)) = \sum_{i \in \mathcal{I}} U_i(\boldsymbol{x}_i(t)) - \sum_{j \in \mathcal{G}} \sum_{h \in \mathcal{H}_t} C_j^{\text{con}}\left(p_j^{\text{con}}(h)\right) - \sum_{j \in \mathcal{G}} D_j\left(\boldsymbol{p}_j^{\text{ren}}(t)\right). \tag{20}$$

The DNO is responsible for managing the market as well as securing the operation of the power network. A linearized ac power flow model [37] can be used to determine the bus voltages and branch flows in a distribution network. Let $\boldsymbol{p}(h) = (p_b(h),\, b \in \mathcal{I} \cup \mathcal{G})$ and $\boldsymbol{q}(h) = (q_b(h),\, b \in \mathcal{I} \cup \mathcal{G})$ denote the vectors of injected active and reactive powers to all buses in time slot h. We define the grid-wide bus voltage vector $\boldsymbol{v}(h) = (v_b(h),\, b \in \mathcal{I} \cup \mathcal{G})$ in time slot h. In Appendix B, we show that there exist predetermined matrices $\boldsymbol{R}$ and $\boldsymbol{X}$, and vector $\boldsymbol{w}_v$, such that $\boldsymbol{v}(h) = \boldsymbol{R}\boldsymbol{p}(h) + \boldsymbol{X}\,\boldsymbol{q}(h) + \boldsymbol{w}_v$. The elements of matrices $\boldsymbol{R}$ and $\boldsymbol{X}$ depend on the admittance matrix of the network. All elements of the vector $\boldsymbol{w}_v$ are zero, except the element correspond to the voltage magnitude of the slack bus, which is set to 1 pu. For each bus b, we have $v_b^{\min} \leq v_b(h) \leq v_b^{\max}$. With the matrix notation, we have

$$\boldsymbol{v}^{\min} \leq \boldsymbol{R}\boldsymbol{p}(h) + \boldsymbol{X}\boldsymbol{q}(h) + \boldsymbol{w}_v \leq \boldsymbol{v}^{\max}, \quad h \in \mathcal{H}_t. \tag{21}$$

We also consider the apparent power flow limits of the branches. In Appendix B, we determine the linearized model for the active power flow $p_{rs}^{\text{flow}}(h)$ and reactive power flow $q_{rs}^{\text{flow}}(h)$ through line $(r,s) \in \mathcal{L}$ in time slot h. The apparent power flow $s_{rs}(h)$ through line (r,s) is upper bounded by $s_{rs}^{\max}$, which implies that the feasible real and reactive powers

1949-3029 (c) 2018 IEEE. Personal use is permitted, but republication/redistribution requires IEEE permission. See http://www.ieee.org/publications_standards/publications/rights/index.html for more information.

This article has been accepted for publication in a future issue of this journal, but has not been fully edited. Content may change prior to final publication. Citation information: DOI 10.1109/TSTE.2018.2815502, IEEE Transactions on Sustainable Energy

are bounded by a circle. To linearize the constraint, we use a piecewise approximation of the circular boundary by a regular polygon with central angle α. In Appendix B, we obtain constraint $p_{rs}^{\text{flow}}(h)\cos(m\alpha) + q_{rs}^{\text{flow}}(h)\sin(m\alpha) \leq s_{rs}^{\max}$, for line $(r,s) \in \mathcal{L}$, where $m = 0, \ldots, 2\pi/\alpha$. We also express $p_{rs}^{\text{flow}}(h)$ and $q_{rs}^{\text{flow}}(h)$ in terms of the vectors of active and reactive power injections. We obtain the following equivalent set of constraints for the branches' power flow limit:

$$\boldsymbol{S}_m\, \boldsymbol{p}(h) + \widetilde{\boldsymbol{S}}_m\, \boldsymbol{q}(h) + \widetilde{\boldsymbol{w}}_m \leq \boldsymbol{s}^{\max}, \quad h \in \mathcal{H}_t, \tag{22}$$

where matrices $\boldsymbol{S}_m$ and $\widetilde{\boldsymbol{S}}_m$, and vector $\widetilde{\boldsymbol{w}}_m$ depend on the values of α, m, and the network admittance matrix.

The DNO considers the impact of renewable generation uncertainty on the technical operation of the network. The variation in the renewable generation can result in an unpredicted voltage rise/drop. The DNO can curtail the renewable generation surplus, and thus the voltage rise can be avoided with almost no cost. However, in the case of generation shortage, the DNO must perform some emergency actions, such as operating the costly backup generators. Hence, the voltage drop can be considered as an acceptable operational metric to study the renewable generation shortage. We use $\boldsymbol{v}(h) = \boldsymbol{R}\,\boldsymbol{p}(h) + \boldsymbol{X}\,\boldsymbol{q}(h) + \boldsymbol{w}_v$ to obtain the voltage drop. In the worst-case scenario, if the renewable generation levels vary from the predicted value $\boldsymbol{p}^{\text{ren}}(h)$ to the minimum level $\boldsymbol{p}^{\text{min,ren}}(h)$ and the conventional generation levels increase from $p_j^{\text{con}}(h)$ to the reserved capacity $F(q_j^{\text{con}}(h))$, then the vector of voltage drops at all buses is obtained as

$$\Delta\boldsymbol{v}(h) = \boldsymbol{R}\,\left(\boldsymbol{p}^{\text{ren}}(h) - \boldsymbol{p}^{\text{min,ren}}(h) - (\mathcal{F}(\boldsymbol{q}(h)) - \boldsymbol{p}^{\text{con}}(h))\right).$$

The DNO aims to ensure $\boldsymbol{v}^{\min} \leq \boldsymbol{v}(h) + \Delta\boldsymbol{v}(h)$, $h \in \mathcal{H}_t$, which can be expressed as

$$\begin{aligned}\boldsymbol{v}^{\min} \leq\, & \boldsymbol{R}\,\boldsymbol{p}(h) + \boldsymbol{X}\,\boldsymbol{q}(h) + \boldsymbol{w}_v + \boldsymbol{R}\left(\boldsymbol{p}^{\text{ren}}(h) - \boldsymbol{p}^{\text{min,ren}}(h)\right.\\ & \left. - (F(\boldsymbol{q}(h)) - \boldsymbol{p}^{\text{con}}(h))\right).\end{aligned} \tag{23}$$

Let $\boldsymbol{y}(t) = (\boldsymbol{\rho}(t), \boldsymbol{\varrho}(t), \boldsymbol{\beta}(t))$ denote the vector of price signals. The DNO's centralized problem is

$$\underset{\boldsymbol{x}(t),\,\boldsymbol{y}(t)}{\text{maximize}}\ f^{\text{DNO}}(\boldsymbol{x}(t)) \tag{24a}$$

$$\text{subject to constraints (21)}-\text{(23)}, \tag{24b}$$

$$\boldsymbol{x}_j(t) = \mathcal{B}_j(\boldsymbol{\rho}_j(t), \boldsymbol{\varrho}_j(t), \boldsymbol{\beta}_j(t)),\ j \in \mathcal{G}, \tag{24c}$$

$$\boldsymbol{x}_i(t) = \mathcal{B}_i(\boldsymbol{\rho}_j(t)), \qquad i \in \mathcal{I}. \tag{24d}$$

Inequality (23) guarantees that the bus voltages remain at their safe limits, even if the actual renewable generation profile deviates from its predicted generation profile. That is, the solution to problem (24) remains feasible even with the renewable generation shortage. The optimal decisions of the entities are included into problem (24) through constraints (24c) and (24d), i.e., the DNO takes into account the reaction of the entities towards any price signals and takes it into consideration when making decisions in a centralized manner. This constitutes a *bi-level* optimization problem, where the network operator solves the outer level and sends the signals $\boldsymbol{y}(t)$ to all entities. Each entity responds with its optimal strategy by solving local problems (8) and (18). Problem (24) is difficult to be solved due to the nonconvexity of constraints (24c) and (24d). We reformulate (24) as a convex optimization problem with a price signal design.

We relax (24c) and (24d) and replace them with the feasibility requirements $\boldsymbol{x}_j(t) \in \mathcal{X}_j(t)$, $j \in \mathcal{G}$ and $\boldsymbol{x}_i(t) \in \mathcal{X}_i(t)$, $i \in \mathcal{I}$, which are convex. For future development, we express the inequalities (21)−(23) in the form of $\sum_{b\in\mathcal{I}\cup\mathcal{G}} \boldsymbol{A}_b\boldsymbol{x}_b(t) - \boldsymbol{c} \preceq 0$. The convex relaxation form of (24) is as follows:

$$\underset{\boldsymbol{x}(t)}{\text{maximize}}\ f^{\text{DNO}}(\boldsymbol{x}(t)) \tag{25a}$$

$$\text{subject to} \sum_{b\in\mathcal{I}\cup\mathcal{G}} \boldsymbol{A}_b\,\boldsymbol{x}_b(t) - \boldsymbol{c} \preceq 0, \tag{25b}$$

$$\boldsymbol{x}_j(t) \in \mathcal{X}_j(t), \qquad j \in \mathcal{G}, \tag{25c}$$

$$\boldsymbol{x}_i(t) \in \mathcal{X}_i(t), \qquad i \in \mathcal{I}. \tag{25d}$$

Problem (25) is a *single-level* convex optimization problem and does not include the price vector $\boldsymbol{y}(t)$ as the decision variable. It is not a trivial fact that there exist price signals $\boldsymbol{y}^*(t) = (\boldsymbol{\rho}^*(t), \boldsymbol{\varrho}^*(t), \boldsymbol{\beta}^*(t))$ such that constraints (24c) and (24d) are satisfied. We will prove that such price signals exist and the relaxation gap between problems (24) and (25) is zero.

IV. Decentralized Algorithm Design

In this section, we first determine the price signals to close the gap between problems (24) and (25). Then, we propose a dual decomposition-based decentralized algorithm that provably converges to solution of problem (25). Finally, we modified our proposed algorithm to an ADMM-based algorithm to improve the convergence rate.

Consider the global optimal point of problem (25). Let $\overline{\lambda}_b^*(h)$ and $\underline{\lambda}_b^*(h)$ denote the dual variables associated with the upper bound and lower bound in constraint (21) for bus b, respectively. Let $\mu_{m,l}^*(h)$ denote the dual variables associated with the constraint (22) for line $l \in \mathcal{L}$ and $m = 0, \ldots, 2\pi/\alpha$. Let $\gamma_b(h)$ denote the dual variable associated with constraint (23) for bus b. Consider the following theorem.

Theorem 1: The gap between problems (24) and (25) is zero if and only if for $i \in \mathcal{I}$, $j \in \mathcal{G}$, $h \in \mathcal{H}_t$, the DNO sets

$$\begin{aligned}\rho_i^*(h) = & \sum_{b\in\mathcal{I}\cup\mathcal{G}} \left(\overline{\lambda}_b^*(h) - \underline{\lambda}_b^*(h) - \gamma_b^*(h)\right)\\ & \left(\boldsymbol{R}_{b,i} + \boldsymbol{X}_{b,i}\,\text{sgn}(\phi_i)\sqrt{\frac{(1-\phi_i^2)}{\phi_i^2}}\right) + \sum_{l\in\mathcal{L}} \mu_{m,l}^*(h)\\ & \left(\boldsymbol{S}_{m,l,i} + \widetilde{\boldsymbol{S}}_{m,l,i}\,\text{sgn}(\phi_i)\sqrt{\frac{(1-\phi_i^2)}{\phi_i^2}}\right),\end{aligned} \tag{26a}$$

$$\begin{aligned}\rho_j^*(h) = & \sum_{b\in\mathcal{I}\cup\mathcal{G}} \left(\overline{\lambda}_b^*(h) - \underline{\lambda}_b^*(h)\right)\boldsymbol{R}_{b,j}\\ & + \sum_{l\in\mathcal{L}} \mu_{m,l}^*(h)\,\boldsymbol{S}_{m,l,j},\end{aligned} \tag{26b}$$

$$\begin{aligned}\varrho_j^*(h) = & \sum_{b\in\mathcal{I}\cup\mathcal{G}} \left(\overline{\lambda}_b^*(h) - \underline{\lambda}_b^*(h) - \gamma_b^*(h)\right)\boldsymbol{X}_{b,j}\\ & + \sum_{l\in\mathcal{L}} \mu_{m,l}^*(h)\,\widetilde{\boldsymbol{S}}_{m,l,j},\end{aligned} \tag{26c}$$

$$\beta_j^*(h) = \sum_{b\in\mathcal{I}\cup\mathcal{G}} \gamma_b^*(h)\boldsymbol{R}_{b,j}. \tag{26d}$$

1949-3029 (c) 2018 IEEE. Personal use is permitted, but republication/redistribution requires IEEE permission. See http://www.ieee.org/publications_standards/publications/rights/index.html for more information.

This article has been accepted for publication in a future issue of this journal, but has not been fully edited. Content may change prior to final publication. Citation information: DOI 10.1109/TSTE.2018.2815502, IEEE Transactions on Sustainable Energy

The proof can be found in Appendix C. It suggests a decentralized algorithm to find the solution to (25).

A. Dual Decomposition-based Decentralized Algorithm

We propose Algorithm 1 that can be executed by the load aggregators, generators, and DNO. In Algorithm 1, when the current time slot t begins, each load aggregator i determines the power consumption profile $\boldsymbol{e}^*_{a,i}(t)$ of the awake appliances $a \in \mathcal{A}_i^{\text{awake}}(t)$. Each generator j obtains the profiles of active and reactive powers $\boldsymbol{p}_j^{*,\text{con}}(t)$ and $\boldsymbol{q}_j^{*,\text{con}}(t)$ of its conventional unit as well as the offered generation profile $\boldsymbol{p}_j^{*,\text{ren}}(t)$ of its renewable plant. The entities apply their scheduling decisions for the current time slot t and use the obtained scheduling decisions for the upcoming time slots $h \geq t+1$ as an *initial* point. Algorithm 1 is executed in an iterative fashion. Let k denote the iteration index. Fig. 4 shows the interactions among generators, load aggregators, and DNO in Algorithm 1. Our algorithm involves the initiation and market trading phases.

• *Initiation phase*: Lines 1 to 9 describe the initiation phase.

• *Market trading phase*: The loop involving Lines 10 to 17 describes this phase, which includes the following parts:

a) Information exchange: In Line 11, each load aggregator i uses (16) to obtain its demand profile $\boldsymbol{l}_i^k(t) = (l_i^k(h), h \in \mathcal{H}_t)$, and sends to the DNO. Each generator j sends the profiles $\boldsymbol{p}_j^{\text{con},k}(t)$, $\boldsymbol{q}_j^{\text{con},k}(t)$, and $\boldsymbol{p}_j^{\text{ren},k}(t)$ to the DNO.

b) DNO's update: In Line 12, the DNO receives the updated vector $\boldsymbol{z}^k(t)$ from the entities. Let $\Lambda^k(t) = (\overline{\boldsymbol{\lambda}}^k(t), \underline{\boldsymbol{\lambda}}^k(t), \boldsymbol{\mu}^k(t), \boldsymbol{\gamma}^k(t))$ denote the vector of grid-wide dual variables in iteration k. The DNO updates $\Lambda^k(t)$ as follows:

$$\Lambda^{k+1}(t) = \left[\Lambda^k(t) + \epsilon^k \left(\sum_{b\in\mathcal{I}\cup\mathcal{G}} \boldsymbol{A}_b\, \boldsymbol{x}_b^k(t) - \boldsymbol{c}\right)\right]^+, \quad (27)$$

where $[\cdot]^+$ is the projection onto the nonnegative orthant and ϵ^k is the stepsize in iteration k. In Line 13, the DNO uses (26a)−(26d) to compute the updated prices $\boldsymbol{\rho}^{k+1}(t)$ and $\boldsymbol{\varrho}^{k+1}(t)$ and penalties $\boldsymbol{\beta}^{k+1}(t)$ for all buses.

c) Generator's update: Generator j receives $\boldsymbol{\rho}_j^{k+1}(t)$, $\boldsymbol{\varrho}_j^{k+1}(t)$ and $\boldsymbol{\beta}_j^{k+1}(t)$ from the DNO. In Line 14, it updates its strategy $\boldsymbol{x}_j^k(t) = (\boldsymbol{p}_j^{\text{con},k}(t), \boldsymbol{q}_j^{\text{con},k}(t), \boldsymbol{p}_j^{\text{ren},k}(t))$ by solving its local problem (8). This problem is a convex optimization and can be solved efficiently.

d) Load aggregator's update: Load aggregator i receives $\rho_i^{k+1}(h)$, $h \in \mathcal{H}_t$ from the DNO. In Line 15, it updates it strategy $\boldsymbol{x}_i^{k+1}(t)$ by solving its local problem in (18) which is a convex optimization problem.

e) Step size update: We use a *nonsummable diminishing* step size, i.e., $\lim_{k\to 0} \epsilon^k = 0$, $\sum_k \epsilon^k = \infty$, and $\sum_k (\epsilon^k)^2 < \infty$. In Line 16, the step size is updated.

B. ADMM-based Decentralized Algorithm

Algorithm 1 is based on the dual iterative method and it is guaranteed to converge to the global optimal solution to (25) (or (24)) for the non-summable diminishing step size [28, Prop. 5.2.1] and [38, Sec. 3.5, Prop. 5.4]. However, the convergence of such a method often tends to be slow in practice. Its convergence rate for strongly convex problems is $O(1/\sqrt{k})$ [28]. Another effective distributed approach is based on the ADMM. The ADMM-based algorithm has attracted attention in the literature (e.g., in [14]–[16]) due to its higher convergence rate compared to the dual decomposition technique. The commonly used form of the ADMM approach is the variable splitting ADMM algorithm [29, Algorithm 1]. Introducing splitting variables can substantially increase the number of variables and constraints. To overcome this issue, we use a Jacobi-type scheme that updates all the variable blocks in parallel. In the following, we develop an algorithm based on the PJ-ADMM [29, Algorithm 4] with prox-linear method [39] to solve problem (25).

Algorithm 1 Decentralized Energy Market Trading Algorithm.

1: Set $k := 1$ and $\xi_1 = \xi_2 := 10^{-3}$.
2: **If** $t = 1$
3: Each load aggregator $i \in \mathcal{I}$ randomly initializes its users' appliances load profile $\boldsymbol{e}_i^1(t)$.
4: Each generator $j \in \mathcal{G}$ randomly initializes its conventional generation profiles $\boldsymbol{p}_j^{\text{con},1}(t)$ and $\boldsymbol{q}_j^{\text{con},1}(t)$.
5: Each generator j sets the presumed generation levels to $p_j^{\text{ren},1}(h) = p_j^{\text{avg,ren}}(h)$ for $h \in \mathcal{H}_t$.
6: DNO sets $v_b^1(h) = 1$ pu, $\delta_b^1 = 0$, $b \in \mathcal{I}\cup\mathcal{G}$, $h \in \mathcal{H}_t$, and $\Lambda^1(t) = \mathbf{0}$.
7: **Else if** $t > 1$
8: Load aggregators, generators, and DNO initialize their decision variables with their most updated values in the equilibrium at time slot $t-1$.
9: **End if**
10: **Repeat**
11: Each load aggregator i and generator j sends its load profile $\boldsymbol{l}_i^k(t)$ and generation profiles $\boldsymbol{p}_j^{\text{con},k}(t)$, $\boldsymbol{q}_j^{\text{con},k}(t)$, and $\boldsymbol{p}_j^{\text{ren},k}(t)$ to the DNO.
12: DNO obtains vector $\Lambda^{k+1}(t)$ using (29).
13: DNO uses (26a)−(26d) to compute the updated values of control signals $\boldsymbol{\rho}^{k+1}(t)$, $\boldsymbol{\varrho}^{k+1}(t)$, and $\boldsymbol{\beta}^{k+1}(t)$, and sends the control signals to the corresponding entity in each bus.
14: Each generator j updates its decision vector.
15: Each load aggregator i updates its load profile.
16: $k := k+1$. The step size is updated.
17: **Until** $|\boldsymbol{\delta}_b^k(t) - \boldsymbol{\delta}_b^{k-1}(t)| \leq \xi_1$, $|\boldsymbol{v}_b^k(t) - \boldsymbol{v}_b^{k-1}(t)| \leq \xi_2$.

First, we develop the augmented Lagrangian of problem (25) with the augmented term $\frac{\tau^{\text{a}}}{2}\left|\left|\boldsymbol{A}\,\boldsymbol{x}(t) - \boldsymbol{c}\right|\right|_2^2$, where $\tau^{\text{a}} > 0$ is a weight coefficient. Next, we decompose the augmented Lagrangian into the local problems for the load aggregators and generators. Consider iteration k of Algorithm 1. For the prox-linear method [39], we add the proximal term $\frac{\tau_b^{\text{p}}}{2}\left|\left|\boldsymbol{x}_b(t) - \boldsymbol{x}_b^k(t)\right|\right|^2$ to the objective function of the local problem associated with bus $b \in \mathcal{G}\cup\mathcal{I}$, where $\tau_b^{\text{p}} > 0$ is the proximal parameter. The price signals $\boldsymbol{y}_b^k(t) = (\boldsymbol{\rho}_b^k(t), \boldsymbol{\varrho}_b^k(t), \boldsymbol{\beta}_b^k(t))$ for bus $b \in \mathcal{G}\cup\mathcal{I}$ in (26a)−(26d) are modified as follows:

$$\widetilde{\boldsymbol{y}}_b^k(t) = \boldsymbol{y}_b^k(t) + \tau^{\text{a}} \boldsymbol{A}_b^{\text{T}} \left[\sum_{b'\in\mathcal{I}\cup\mathcal{G}} \boldsymbol{A}_{b'}\, \boldsymbol{x}_{b'}^k(t) - \boldsymbol{c}\right]^+. \quad (28)$$

1949-3029 (c) 2018 IEEE. Personal use is permitted, but republication/redistribution requires IEEE permission. See http://www.ieee.org/publications_standards/publications/rights/index.html for more information.

This article has been accepted for publication in a future issue of this journal, but has not been fully edited. Content may change prior to final publication. Citation information: DOI 10.1109/TSTE.2018.2815502, IEEE Transactions on Sustainable Energy

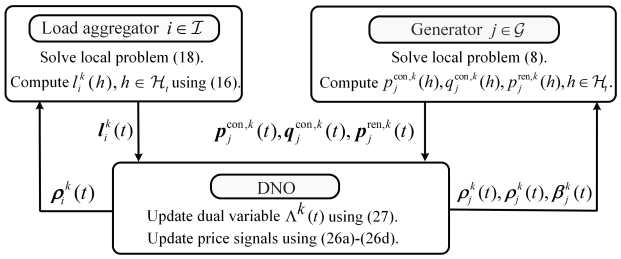

Figure 4. Interactions among generators, load aggregators, and DNO.

The DNO's update in (29) is modified to

$$\Lambda^{k+1}(t) = \left[\Lambda^k(t) + \zeta\, \tau^{\text{a}} \left(\sum_{b \in \mathcal{I} \cup \mathcal{G}} \boldsymbol{A}_b\, \boldsymbol{x}_b^k(t) - \boldsymbol{c} \right)\right]^+, \quad (29)$$

where $0 < \zeta < 1$ is a damping parameter. The modified algorithm has global convergence with rate $O(1/k)$ under the condition $\tau_b^{\text{p}} > \tau^{\text{a}} ||\boldsymbol{A}_b||^2 \frac{|\mathcal{G} \cup \mathcal{I}|}{2-\zeta}$ for all buses [29, Lemma 2.2].

V. Performance Evaluation

In this section, we evaluate the performance of our proposed decentralized algorithm on the IEEE 123-bus distribution test feeder shown in Fig. 5. The original test system is unbalanced. We consider only phase a, and consider the balanced configuration, where all switched are open. The trading horizon is one day with $H = 96$, 15-minute time slots. The lines data for the test system can be found in [40]. The limit for the apparent power flow of branches is 1.05 pu. Parameter α is set to $15°$. The limits on the bus voltages are 0.96 pu and 1.04 pu. The test system has no generator in its original structure. We modify this feeder by adding 5 generators in different buses. For the quadratic cost functions of the conventional units of generators $j \in \mathcal{G}$, the coefficients a_{j2} and a_{j1} are randomly chosen from the intervals $[0.01\,\$/(\text{kW})^2, 0.025\,\$/(\text{kW})^2]$ and $[0.2\,\$/\text{kW}, 0.4\,\$/\text{kW}]$, respectively, and coefficient a_{j0} is set to zero. We use the data in [30, Ch. 5.4] to model the loading capability of the generators. We assume that three generators have PV panels and two generators have wind turbine. To obtain the samples for the output power of the renewables, we scale down the available historical data from Ontario, Canada power grid database [41], from November 1 to November 21, 2016. The weight coefficients d_j, $j \in \mathcal{G}$ are chosen randomly chosen from the interval $[0.02\,\$/(\text{kWh})^2, 0.05\,\$/(\text{kWh})^2]$.

We assume that each load aggregator serves between 30 to 60 residential households. To model the demand of each load aggregator, we assume that each residential customer has the major appliances including EV, dish washer, washing machine, dryer (as type 1), TV, PC, oven (as type 2), lighting, refrigerator, freezer, and fan (as type 3). The nominal power of the appliances can be found in [42]. For each appliance, the awaking time probability distribution $\boldsymbol{p}_a(h)$ is set as a truncated normal distribution lower bounded by zero. Its mean value is chosen at random from 8 pm to 6 am for the EV, 12 am to 12 pm for the refrigerator and freezer, and 10 am to 10 pm for other appliances. The standard deviation is set to 45 minutes. When an appliance becomes awake, its scheduling window is selected between the awake time to the end of the operation cycle, $\mathcal{H}$. The length of the scheduling windows are uniformly chosen at random from set $\{4\,\text{hr}, 5\,\text{hr}, \ldots, 10\,\text{hr}\}$ for the EVs, $\{7\,\text{hr}, 2\,\text{hr}, \ldots, 23\,\text{hr}\}$ for the the refrigerator and freezer, and $\{1\,\text{hr}, 2\,\text{hr}, \ldots, 5\,\text{hr}\}$ for other appliances.

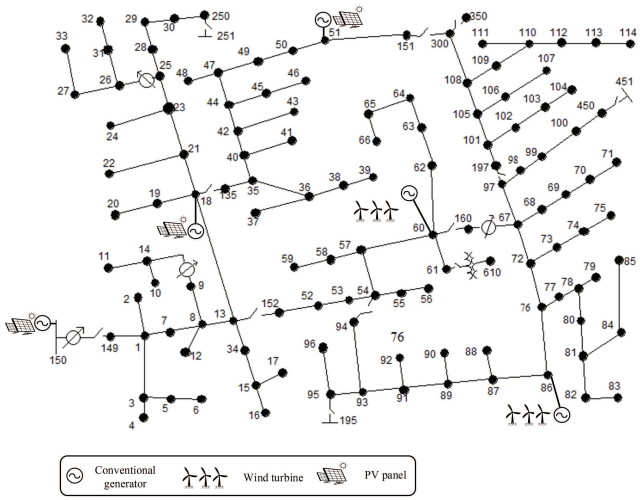

Figure 5. A modified IEEE 123-bus test system [40] with 5 generators and 118 load aggregators. The generators in buses 18, 51, and 150 have PV panels, and the generators in buses 60 and 86 have wind turbines.

We use the logarithmic utility function $u(\cdot)$. For appliances of type 1, constant $\kappa_{a,i}$ is randomly chosen from $[0.5\,\$/\text{kW}, 1.5\,\$/\text{kW}]$. For appliances of type 2, *time dependent* coefficients $\kappa_{a,i}(h)$ and $\kappa'_{a,i}(h)$ are randomly chosen from intervals $[0.5\,\$/\text{kW}, 1.5\,\$/\text{kW}]$ and $[0.1\,\$/\text{kW}, 0.3\,\$/\text{kW}]$, respectively. For appliances of type 3, *constants* $\kappa_{a,i}$ and $\kappa'_{a,i}$ are randomly chosen from intervals $[0.5\,\$/\text{kW}, 1.5\,\$/\text{kW}]$ and $[0.1\,\$/\text{kW}, 0.3\,\$/\text{kW}]$, respectively. For the benchmark scenario, we consider a system without renewable generation for the generators and without demand response for the load aggregators, and thus the users operate their appliances right after they become awake with the nominal power consumption. We use MOSEK solver and perform simulations using Matlab R2016b, CVX in a PC with processor Intel(R) Core(TM) i7-3770K CPU@3.5 GHz.

A. Load Aggregators' and Generators' Strategy

Each load aggregator executes Algorithm 1 to schedule the appliances of its users. Fig. 6 shows the total load profiles of the load aggregators in buses 17, 23, 90, and 110 in the benchmark scenario and the scenario with load scheduling. Peak shaving can be observed in the load profiles. Results for *all* load aggregators verify that by executing Algorithm 1, the peak load demand is reduced by 19.73% on average. Load scheduling is performed by each load aggregator with the goal of increasing the profit in (17). Fig. 7 shows that the profit of the load aggregators 17, 23, 90, and 110 increases with demand response. Specifically, results show that the profit for *all* load aggregators is increased by 22.34% on average, since they can observe the price fluctuations and modify the appliances' schedule accordingly. Moreover with renewable generation, the electricity price is reduced. Thus, the load aggregators can benefit from lower prices during the day.

1949-3029 (c) 2018 IEEE. Personal use is permitted, but republication/redistribution requires IEEE permission. See http://www.ieee.org/publications_standards/publications/rights/index.html for more information.

This article has been accepted for publication in a future issue of this journal, but has not been fully edited. Content may change prior to final publication. Citation information: DOI 10.1109/TSTE.2018.2815502, IEEE Transactions on Sustainable Energy

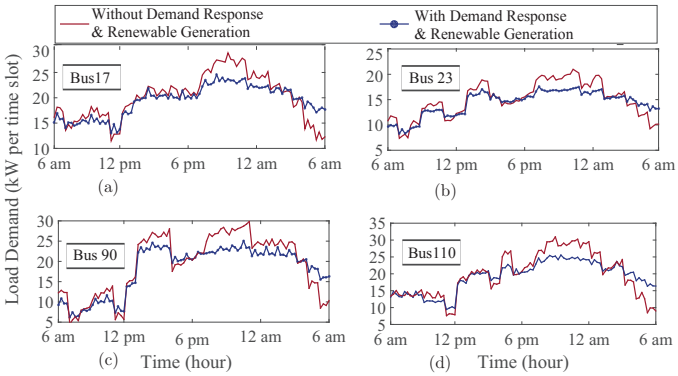

Figure 6. The profiles of total load demand during one day with 96 time slots for buses 17, 23, 90, and 110 with and without demand response and renewable generation.

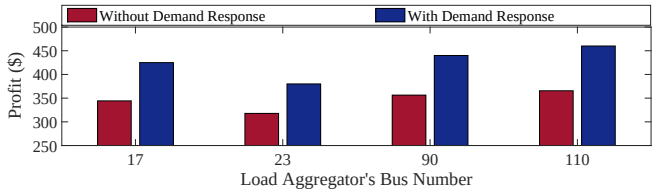

Figure 7. The profit for load aggregators with and without demand response and renewable generation.

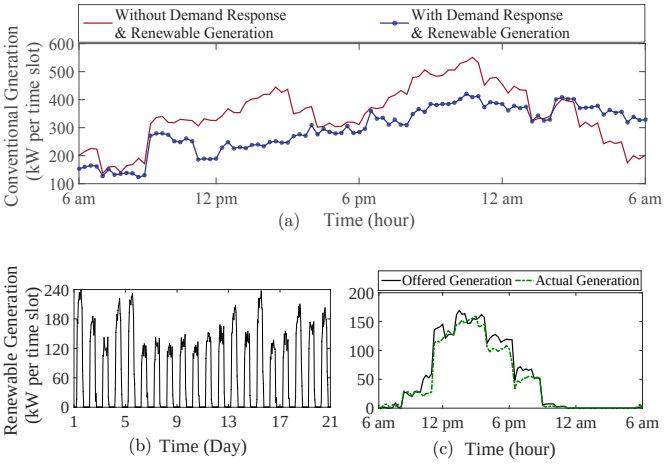

Figure 8. (a) The generation of the conventional unit of the generator in bus 18; (b) the PV panel's historical data samples; and (c) the offered and actual generation profiles of the PV panels installed at bus 18.

The generators can benefit from the renewable units' production and users' load scheduling to smooth out their conventional generation profiles; thereby reducing their generation cost during the peak hours. For example, Fig. 8 (a) shows the conventional generation profile of the generator in bus 18. With renewable generation and demand response, the peak generation level is reduced from 537 kW to 413 kW per time slot (i.e. 24% reduction). This generator has a PV panel with the historical generation record shown in Fig. 8 (b). The generator executes Algorithm 1 and responds to the penalties $\boldsymbol{\beta}_j(t)$ from the DNO in each time slot to set the generation level for its PV panel. The uncertainty budget is set to $\Delta_j(t) = \sqrt{\mathcal{H}_t}$. Fig. 8 (c) shows the result for the offered and

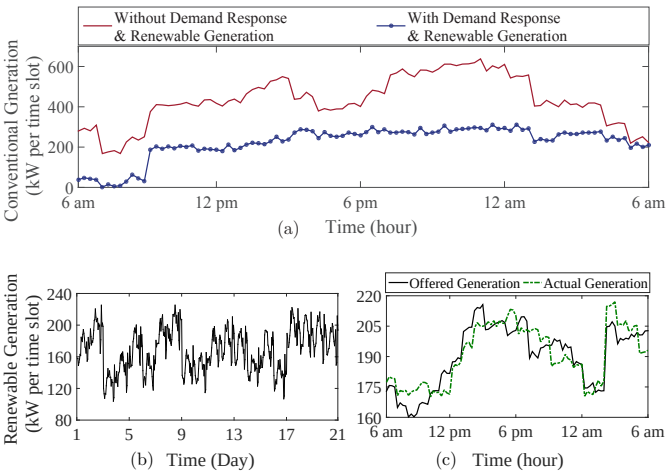

Figure 9. (a) The generation of the conventional unit of the generator in bus 60; (b) the wind turbine's historical data samples; and (c) the offered and actual generation profiles of the wind turbines installed at bus 60.

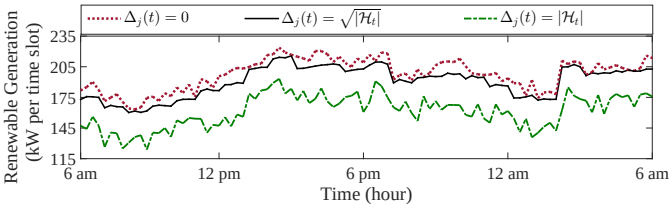

Figure 10. The offered renewable generation of the generator in bus 60 for different values of the uncertainty budget $\Delta_j(t)$.

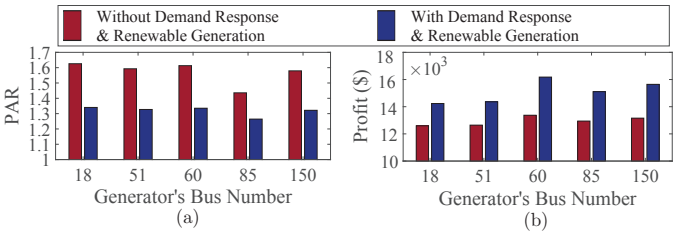

Figure 11. (a) The PAR in the generation and (b) the profit of the generators.

actual renewable generations. The offers may not be equal to the actual production; however by considering the generation uncertainty, the offered generation results in the optimal risk of energy shortage in bus 18. Fig. 9 (a) shows the conventional generation profile of the generator in bus 60. The reduction in the peak generation can be observed. This generator has a wind turbine with the historical generation record shown in Fig. 9 (b). Fig. 9 (c) shows the offered and actual generation profiles for the wind turbine in bus 60.

The offers for the generation of renewable units mainly depends on the uncertainty budget of the generators. In particular, Fig. 10 shows that when parameter $\Delta_j(t)$ in (5) is zero, then the generator in bus 60 offers $p_j^{\text{ren}}(h) = p_j^{\text{avg,ren}}(h)$, $h \in \mathcal{H}_t$. As $\Delta_j(t)$ increases, the size of the uncertainty set enlarges. In [32], $\Delta_j(t) \approx \sqrt{|\mathcal{H}_t|}$ is suggested and we can observe that the offered generation is slightly lower than the average generation levels. If $\Delta_j(t) = |\mathcal{H}_t|$, then the generator becomes risk-averse and offers a relatively lower generation level to the market. Although with $\Delta_j(t) = |\mathcal{H}_t|$, the generator will pay

1949-3029 (c) 2018 IEEE. Personal use is permitted, but republication/redistribution requires IEEE permission. See http://www.ieee.org/publications_standards/publications/rights/index.html for more information.

This article has been accepted for publication in a future issue of this journal, but has not been fully edited. Content may change prior to final publication. Citation information: DOI 10.1109/TSTE.2018.2815502, IEEE Transactions on Sustainable Energy

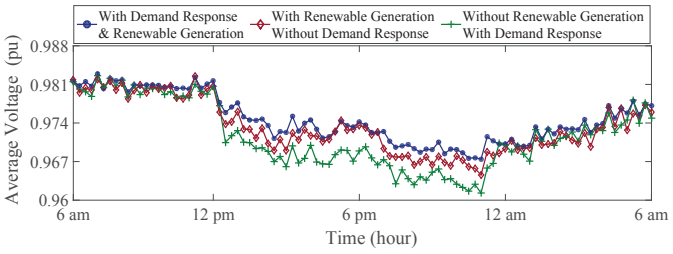

Figure 12. Average voltage magnitude of all buses during the day with and without renewable generation and demand response program.

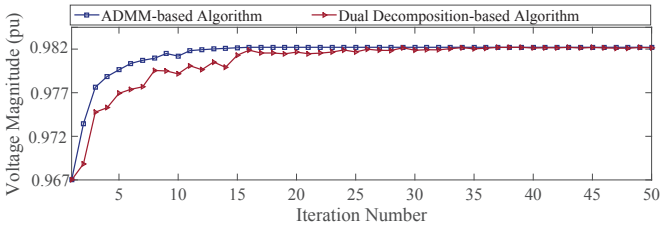

Figure 13. The convergence of average voltage magnitude at 12 pm.

lower penalty for the generation shortage, this is not preferable because the generator will have a significantly lower revenue from selling renewable generation. To quantify the strategic behaviour of the generators, we consider the PAR of the generation. Fig. 11 (a) shows that the PAR is reduced for the generators by 16.9% on average. A lower PAR means a lower generation cost, and thus a higher profit. Fig. 11 (b) shows that the generators' profit is increased by 15.2% on average.

B. DNO's Strategy for the Voltage Profile

We study how the demand response and renewable generation affect the voltage profile. We consider the average voltage magnitude of all buses in different time slots for three scenarios: (i) the scenario with renewable generation and demand response, (ii) the scenario with renewable generation and without demand response, and (iii) the scenario without renewable generation and with demand response. Fig. 12 shows that the average voltage is higher in the first scenario. The demand response deployment results in a lower peak load, and thus a lower voltage drop in different buses. The DNO also takes into account constraint (23) to ensure sufficient margin for the voltage drop. The DNO aims to guarantee the network safe operation in case of high renewable generation shortages. Hence in the first scenario, the DNO operates the network with a larger voltage margin from the lower bound 0.96 pu. In the second scenario, we can observe a lower voltage levels specially during the intervals [12 pm, 5pm] and [7 pm, 11 pm]. The reason is the higher demand during these time periods (see Fig. 6) without demand response. In the third scenario, the lack of renewable generation causes the DNO to be certain about the total generation level in the system. Hence, it will operate the system with a smaller voltage margin from 0.96 pu with the goal of reducing the conventional generation levels and achieving a higher social welfare.

C. Algorithm Convergence and Running Time

We study the required number of iterations for convergence of Algorithm 1 with the dual decomposition and PJ-ADMM methods. For instance, we consider the convergence of the average voltage magnitude of all buses at 12 pm. Fig. 13 shows that Algorithm 1 with the dual decomposition converges in about 45 iterations. Whereas, 22 iterations are enough for the convergence of Algorithm 1 with the PJ-ADMM. We also consider six test systems in Table I. All test systems can be found in [40] except the system with 1300 buses, which is a part of 8500-bus test system. In the test networks

Table I
THE AVERAGE NUMBER OF REQUIRED ITERATIONS OF THE DUAL DECOMPOSITION-BASED AND PJ-ADMM-BASED ALGORITHMS.

	Average Number of Requiered Iterations	
Test System	Dual Decomposition-based	PJ-ADMM-based
IEEE 13-bus	15	11
IEEE 34-bus	18	13
IEEE 37-bus	27	16
IEEE 123-bus	41	22
IEEE 1300-bus	139	102
IEEE 8500-bus	191	127

other than IEEE 123-bus system, the number of generators is set to 10% of the number of load aggregators. Half of the generators are equipped with PV panels and the others have wind turbines. The specifications of the generators and load aggregators are set according to the simulation setup. We observe that Algorithm 1 with the PJ-ADMM method converges faster. However, it does not imply that PJ-ADMM method is always preferable to the dual decomposition method. Algorithm 1 with the dual decomposition method leads to a profit maximization subproblems for the entities, which is practical. Whereas, the PJ-ADMM method requires the DNO to *motivate* the entities to add a *proximal* term to their objective functions, which may not be implementable in practice.

Next, we evaluate the scalability of Algorithm 1 by comparing its running time with the centralized algorithm for different test systems. In the centralized algorithm, the DNO solves problem (25). In Fig. 14, we provide the average running time of Algorithm 1 and the centralized approach for six test systems. The centralized algorithm suffers from a high execution time due to the large number of decision variables and constraints. On the other hand, Algorithm 1 is executed by each entity to solve its own local optimization problem with its locally available information in a distributed and parallel fashion. Hence, the number of decision variables for each entity becomes independent of the size of the test system. The overall running time of Algorithm 1 increases almost linearly with the number of buses due to the increase in the required number of iterations for convergence in larger test systems. The running time with the PJ-ADMM is lower due to the smaller number of iterations required to converge.

1949-3029 (c) 2018 IEEE. Personal use is permitted, but republication/redistribution requires IEEE permission. See http://www.ieee.org/publications_standards/publications/rights/index.html for more information.

This article has been accepted for publication in a future issue of this journal, but has not been fully edited. Content may change prior to final publication. Citation information: DOI 10.1109/TSTE.2018.2815502, IEEE Transactions on Sustainable Energy

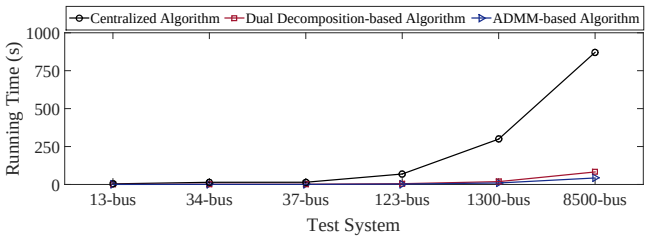

Figure 14. The running time of the centralized and decentralized algorithms.

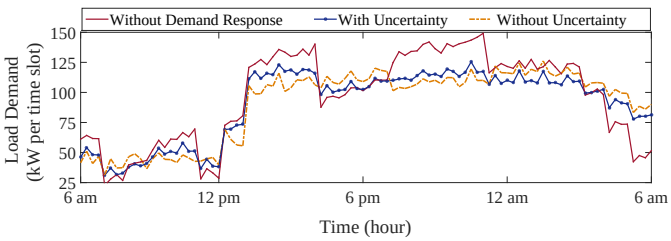

Figure 15. Load scheduling for bus 110 with and without uncertainty.

Table II
THE OPTIMAL VALUE OF THE DNO'S PROBLEM (25) WITH LINEARIZED AC AND FULL AC POWER FLOW MODELS.

	Optimal Objective Value	
Test system	Linearized ac Power Flow	Full ac Power Flow
IEEE 13-bus	14,280.18	14,136.74
IEEE 34-bus	31,449.23	30,954.47
IEEE 37-bus	39,751.48	39,204.61
IEEE 123-bus	124,041.68	121,863.09
IEEE 1300-bus	1,582,458.48	1,538,505.67
IEEE 8500-bus	5,374,020.35	5,218,818.64

D. Linearized ac and Full ac Power Flow Models

We elaborately investigate the approximation in using the linearized AC power flow model. We compare the optimal value of the DNO's problem (25) with the linearized ac power flow and full ac power flow models. We apply semidefinite programming (SDP) to obtain the *global* optimal value of the DNO's problem with the full ac power flow model [43], [44]. The calculation results in Table II show that the optimal value of the DNO's problem with full ac power flow model is lower by about 1.2% (in 13-bus system) to 2.9% (in 8500-bus system) than the optimal value with linearized ac power flow model. A main difference is that the full ac power flow includes the network losses, while the linearized ac power flow is a lossless model. The inclusion of the power losses leads to a higher generation cost and lower bus voltages, and thus a slightly smaller optimal value for the DNO's problem.

E. Impacts of Uncertainties

We also compare the performance of Algorithm 1 for the scenario with uncertainty in the load demand and renewable generation and the scenario with complete information. As an example, we consider the load profile of the load aggregator 110 in Fig. 15. The lack of information makes the load aggregator to be more conservative, since it considers the *worst-case* demand for the currently sleeping appliances in the upcoming time slots. Whereas, when the load aggregator has complete information, it can better manage the appliances especially during the peak hours. The difference between the two load profiles is 3.84%. It shows that using a receding horizon technique can lead to a near-optimal load scheduling compared to the scenario with complete information. The receding horizon technique enables the load aggregator to observe new information and modifies its load estimation at the beginning of every time slot.

VI. CONCLUSION

In this paper, we proposed a decentralized algorithm for energy trading among the load aggregators and generators. We considered the uncertainty in the generation and load. The centralized problem was formulated as a bi-level optimization problem. Convex relaxation techniques were used to convexify the problem. We proved the zero relaxation gap and developed a decentralized the IEEE 123-bus test feeder showed that the proposed algorithm helped the load aggregators and generators by increasing their profit by 23.34% and 15.2% on average, respectively. It also helped the generators to reduce the PAR by 16.9%. Our algorithm converged to the solution of the centralized problem with a significantly lower execution time and a smaller number of iterations. Our algorithm with the PJ-ADMM converged faster compared to the dual decomposition. When compared to the full ac power flow, the optimal objective value with the linearized ac power flow model was smaller by 1.2% to 2.9%. The difference between the scheduled load profiles with and without uncertainty was only 3.84%, which shows the acceptable performance of our algorithm.

ACKNOWLEDGEMENT

J.P.S. Catalão acknowledges the support by FEDER funds through COMPETE 2020 and by Portuguese funds through FCT, under Projects SAICT-PAC/0004/2015 - POCI-01-0145-FEDER-016434, POCI-01-0145-FEDER-006961, UID/EEA/50014/2013, UID/CEC/50021/2013, UID/EMS/00151/2013, and 02/SAICT/2017 - 029803, and also funding from the EU 7th Framework Programme FP7/2007-2013 under GA no. 309048.

APPENDIX

APPENDIX A: THE PROOF OF EQUATION (14)

By definition, with probability $p_a(h)$, $a \in \mathcal{A}_i$, $h \in \mathcal{H}$, each appliance a becomes awake at each time slot $h \in \mathcal{H}$. We use the Bayes rule to compute $p_a(h \mid t)$. We have

$$p_a(h \mid t) = \text{Prob}\{\text{e}_1 | \text{e}_2\} = \frac{\text{Prob}\{\text{e}_2 | \text{e}_1\}\,\text{Prob}\{\text{e}_1\}}{\text{Prob}\{\text{e}_2\}}, \quad (30)$$

where e_1 is the event that the appliance becomes awake in the upcoming time slot $h > t$ and e_2 is the event that the appliance has not become awake until the current time t. The conditional

1949-3029 (c) 2018 IEEE. Personal use is permitted, but republication/redistribution requires IEEE permission. See http://www.ieee.org/publications_standards/publications/rights/index.html for more information.

This article has been accepted for publication in a future issue of this journal, but has not been fully edited. Content may change prior to final publication. Citation information: DOI 10.1109/TSTE.2018.2815502, IEEE Transactions on Sustainable Energy

probability Prob$\{e_2|e_1\}$ is equal to 1, since appliance a is asleep with probability 1 in time t if it becomes awake in the upcoming time slot $h > t$. By definition, Prob$\{e_1\}$ is equal to $p_a(h)$. Prob$\{e_2\}$ is equal to $1-\sum_{h'=1}^{t} p_a(h')$. Substituting these probabilities in (30) completes the proof. ■

Appendix B: Linearized ac Power Flow Model

We use the approach in [37] to formulate the linearized ac power flow model. Let $\delta_b(h)$ denote the voltage phase angle of bus b in time h. Let G_{rs} and B_{rs} denote the real and reactive parts of the entry (r,s) in admittance matrix Y. Let b_{rr} and g_{rr} denote the shunt susceptance and conductance at bus r. The linearized ac power flow can be expressed as [37]

$$\begin{bmatrix}\boldsymbol{p}(h)\\ \boldsymbol{q}(h)\end{bmatrix}=\begin{bmatrix}-\boldsymbol{B}' & \boldsymbol{G}'\\ -\boldsymbol{G} & -\boldsymbol{B}\end{bmatrix}\begin{bmatrix}\boldsymbol{\delta}(h)\\ \boldsymbol{v}(h)\end{bmatrix},\quad h\in\mathcal{H}_t, \tag{31}$$

where the diagonal element (r,r) of matrices $\boldsymbol{B}$ and $\boldsymbol{B}'$ are B_{rr} and $B_{rr}-b_{rr}$, respectively. The non-diagonal elements (r,s) of both $\boldsymbol{B}$ and $\boldsymbol{B}'$ are B_{rs}. The diagonal element (r,r) of matrices $\boldsymbol{G}$ and $\boldsymbol{G}'$ are G_{rr} and $G_{rr}-g_{rr}$, respectively. The non-diagonal elements (r,s) of both $\boldsymbol{G}$ and $\boldsymbol{G}'$ are G_{rs}. The approach is performed around flat voltage profile and negligible angle difference. We exclude the row and column correspond to the slack bus. We invert the remaining matrix equation (31). We add a row and column with all zero elements correspond to the slack bus index. We can write the voltage angles and magnitudes of all buses (including the slack bus) in terms of the injected powers as follows:

$$\begin{bmatrix}\boldsymbol{\delta}(h)\\ \boldsymbol{v}(h)\end{bmatrix}=\begin{bmatrix}\boldsymbol{X}' & \boldsymbol{R}'\\ \boldsymbol{R} & \boldsymbol{X}\end{bmatrix}\begin{bmatrix}\boldsymbol{p}(h)\\ \boldsymbol{q}(h)\end{bmatrix}+\begin{bmatrix}\boldsymbol{w}_\delta\\ \boldsymbol{w}_v\end{bmatrix},\ h\in\mathcal{H}_t, \tag{32}$$

where the elements of matrices $\boldsymbol{R}$, $\boldsymbol{R}'$, $\boldsymbol{X}$, and $\boldsymbol{X}'$ depend on the admittance matrix of the network. All elements of the column vector $\boldsymbol{w}_\delta$ are zero. All elements of the column vector $\boldsymbol{w}_v$ are zero, except the element correspond to the voltage magnitude of the slack bus, which is set to 1 pu. The linearized power flow through line (r,s) can be obtained as:

$$p_{rs}^{\text{flow}}(h)=\frac{R_{rs}(v_r(h)-v_s(h))+X_{rs}(\delta_r(h)-\delta_s(h))}{R_{rs}^2+X_{rs}^2}, \tag{33a}$$

$$q_{rs}^{\text{flow}}(h)=\frac{X_{rs}(v_r(h)-v_s(h))-R_{rs}(\delta_r(h)-\delta_s(h))}{R_{rs}^2+X_{rs}^2}. \tag{33b}$$

We define the vectors $\boldsymbol{p}^{\text{flow}}(h)=(p_{rs}^{\text{flow}}(h),\,(r,s)\in\mathcal{L})$ and $\boldsymbol{q}^{\text{flow}}(h)=(q_{rs}^{\text{flow}}(h),\,(r,s)\in\mathcal{L})$ in time slot h. Equations (33a) and (33b) can be expressed as

$$\begin{bmatrix}\boldsymbol{p}^{\text{flow}}(h)\\ \boldsymbol{q}^{\text{flow}}(h)\end{bmatrix}=\begin{bmatrix}\boldsymbol{L}_\delta & \boldsymbol{L}_v\\ \boldsymbol{L}'_\delta & \boldsymbol{L}'_v\end{bmatrix}\begin{bmatrix}\boldsymbol{\delta}(h)\\ \boldsymbol{v}(h)\end{bmatrix},\quad h\in\mathcal{H}_t, \tag{34}$$

where r-th and s-th elements in the row that corresponds to line $(r,s)\in\mathcal{L}$ for the $|\mathcal{L}|\times|\mathcal{I}\cup\mathcal{G}|$ matrices $\boldsymbol{L}_v$, $\boldsymbol{L}_\delta$, $\boldsymbol{L}'_v$, $\boldsymbol{L}'_\delta$ are $\frac{R_{rs}}{R_{rs}^2+X_{rs}^2}$, $\frac{X_{rs}}{R_{rs}^2+X_{rs}^2}$, $\frac{X_{rs}}{R_{rs}^2+X_{rs}^2}$, and $-\frac{R_{rs}}{R_{rs}^2+X_{rs}^2}$, respectively. Other elements are zero. Combining (32) and (34), we obtain the following matrix equation for the branch flows:

$$\begin{bmatrix}\boldsymbol{p}^{\text{flow}}(h)\\ \boldsymbol{q}^{\text{flow}}(h)\end{bmatrix}=\begin{bmatrix}\widehat{\boldsymbol{L}}_p & \widehat{\boldsymbol{L}}_q\\ \widehat{\boldsymbol{L}}'_p & \widehat{\boldsymbol{L}}'_q\end{bmatrix}\begin{bmatrix}\boldsymbol{p}(h)\\ \boldsymbol{q}(h)\end{bmatrix}+\begin{bmatrix}\widehat{\boldsymbol{w}}_p\\ \widehat{\boldsymbol{w}}_q\end{bmatrix},\ h\in\mathcal{H}_t. \tag{35}$$

The apparent power flow $s_{rs}(h)=\sqrt{p_{rs}^2(h)+q_{rs}^2(h)}$ in line (r,s) is upper bounded by $s_{rs}^{\max}$, which is a circle. To linearize the constraint, we use a piecewise approximation of the boundary by a peripheral regular polygon with central angle α. We have

$$p_{rs}^{\text{flow}}(h)\cos(m\alpha)+q_{rs}^{\text{flow}}(h)\sin(m\alpha)\ \le s_{rs}^{\max}, \tag{36}$$

where $m=0,\ldots,2\pi/\alpha$. Substituting (35) into (36), we obtain

$$\boldsymbol{S}_m\,\boldsymbol{p}(h)+\widetilde{\boldsymbol{S}}_m\,\boldsymbol{q}(h)+\widetilde{\boldsymbol{w}}_m\ \le \boldsymbol{s}^{\max},\quad h\in\mathcal{H}_t, \tag{37}$$

where $\boldsymbol{S}_m=\cos(m\alpha)\widehat{\boldsymbol{L}}_p+\sin(m\alpha)\widehat{\boldsymbol{L}}'_p$, $\widetilde{\boldsymbol{S}}_m=\cos(m\alpha)\widehat{\boldsymbol{L}}_q+\sin(m\alpha)\widehat{\boldsymbol{L}}'_q$, and $\widetilde{\boldsymbol{w}}_m=\cos(m\alpha)\widehat{\boldsymbol{w}}_p+\sin(m\alpha)\widehat{\boldsymbol{w}}_q$. ■

Appendix C: The Proof of Theorem 1

We first develop the Lagrangian of problem (25). Let $\Lambda(t)=(\overline{\boldsymbol{\lambda}}(t),\,\underline{\boldsymbol{\lambda}}(t),\,\boldsymbol{\mu}(t),\,\boldsymbol{\gamma}(t))$ denote the vector of dual variables.

$$\mathcal{L}(\boldsymbol{x}(t),\Lambda(t))=$$
$$f^{\text{DNO}}(\boldsymbol{x}(t))-\Lambda(t)^{\text{T}}\left(\sum_{b\in\mathcal{I}\cup\mathcal{G}}\boldsymbol{A}_b\,\boldsymbol{x}_b(t)-\boldsymbol{c}\right). \tag{38}$$

Now we consider the first-order optimality conditions for (25). For $b\in\mathcal{I}\cup\mathcal{G}$ and all $\boldsymbol{x}_b(t)\in\mathcal{X}_b(t)$, we have

$$\nabla_{\boldsymbol{x}_b(t)}\mathcal{L}(\boldsymbol{x}^*(t),\Lambda^*(t))\left(\boldsymbol{x}_b(t)-\boldsymbol{x}_b^*(t)\right)\le 0. \tag{39}$$

If we write the optimality condition in (39) for $\boldsymbol{x}_i(t)$, $i\in\mathcal{I}$, $\boldsymbol{p}_j^{\text{con}}(t)$, $\boldsymbol{q}_j^{\text{con}}(t)$, and $\boldsymbol{p}_j^{\text{ren}}(t)$, $j\in\mathcal{G}$, then the results will be the optimality conditions for the local problems (8) and (18) with the price signals in (26a)−(26d). As an example, consider load aggregator $i\in\mathcal{I}$. Then, we have

$$\nabla_{\boldsymbol{x}_i(t)}\mathcal{L}(\boldsymbol{x}^*(t),\Lambda^*(t))=$$
$$\nabla_{\boldsymbol{x}_i(t)}\Big(U_i(\boldsymbol{x}_i^*(t))-\Lambda^*(t)^{\text{T}}(\boldsymbol{A}_i\,\boldsymbol{x}_i^*(t))\Big). \tag{40}$$

We can show that the term $\nabla_{\boldsymbol{x}_i(t)}\Lambda^*(t)^{\text{T}}(\boldsymbol{A}_i\,\boldsymbol{x}_i^*(t))$ in (40) can be expressed as $\sum_{h\in\mathcal{H}_t}l_i^*(h)\rho_i^*(h)$, where $\rho_i^*(h)$ is given in (26a). Hence, the optimality condition in (39) for $\boldsymbol{x}_i(t)$, $i\in\mathcal{I}$ is in fact the optimality condition for the local problem (18) with price signal $\rho_i^*(h)$ in (26a), i.e., we have $\boldsymbol{x}_i^*(t)=\mathcal{B}_i(\boldsymbol{\rho}_i^*(t))$. In a similar way, we can show that $\boldsymbol{x}_j^*(t)=\mathcal{B}_j(\boldsymbol{\rho}_j^*(t),\boldsymbol{\varrho}_j^*(t),\boldsymbol{\beta}_j^*(t))$ with the price signals in (26b)−(26d). Hence, the solution to problem (25) with the price signals in (26a)−(26d) is feasible for the original problem (24). Since (25) is the relaxation form of (24), the relaxation gap is zero with price signals in (26a)−(26d). ■

References

[1] M. F. Akorede, H. Hizam, and E. Pouresmaeil, "Distributed energy resources and benefits to the environment," *Renewable and Sustainable Energy Reviews*, vol. 14, no. 2, pp. 724–734, Feb. 2010.

[2] A. Tani, M. B. Camara, and B. Dakyo, "Energy management in the decentralized generation systems based on renewable energy−ultracapacitors and battery to compensate the wind/load power fluctuations," *IEEE Trans. on Industry Applications*, vol. 51, no. 2, pp. 1817–1827, Mar. 2015.

[3] M. F. Akorede, H. Hizam, I. Aris, M. Z. Kadir, and E. Pouresmaeil, "Economic viability of distributed energy resources relative to substation and feeder facilities expansion," in *Proc. of IEEE Int'l Conf. on Power and Energy*, Nov. 2010, pp. 238–242.

1949-3029 (c) 2018 IEEE. Personal use is permitted, but republication/redistribution requires IEEE permission. See http://www.ieee.org/publications_standards/publications/rights/index.html for more information.

This article has been accepted for publication in a future issue of this journal, but has not been fully edited. Content may change prior to final publication. Citation information: DOI 10.1109/TSTE.2018.2815502, IEEE Transactions on Sustainable Energy

[4] S. Bahrami, F. Khazaeli, and M. Parniani, "Industrial load scheduling in smart power grids," in *Proc. of Int'l Conf. and Exhibition on Electricity Distribution*, Stockholm, Sweden, pp. 1–4.

[5] B. Chai, J. Chen, Z. Yang, and Y. Zhang, "Demand response management with multiple utility companies: A two-level game approach," *IEEE Trans. on Smart Grid*, vol. 5, no. 2, pp. 722–731, Mar. 2014.

[6] S. Maharjan, Q. Zhu, Y. Zhang, S. Gjessing, and T. Basar, "Dependable demand response management in the smart grid: A Stackelberg game approach," *IEEE Trans. on Smart Grid*, vol. 4, no. 1, pp. 120–132, Mar. 2013.

[7] R. Deng, Z. Yang, F. Hou, M. Y. Chow, and J. Chen, "Distributed real-time demand response in multiseller-multibuyer smart distribution grid," *IEEE Trans. on Power Systems*, vol. 30, no. 5, pp. 2364–2374, Sept. 2015.

[8] M. Parvania, M. Fotuhi-Firuzabad, and M. Shahidehpour, "ISO's optimal strategies for scheduling the hourly demand response in day-ahead markets," *IEEE Trans. on Power Systems*, vol. 29, no. 6, pp. 2636–2645, 2014.

[9] M. H. Amini, B. Nabi, and M. R. Haghifam, "Load management using multi-agent systems in smart distribution network," in *Proc. of IEEE Power Energy Society General Meeting*, Vancouver, BC, Jul. 2013, pp. 1–5.

[10] L. Gan, N. Li, U. Topcu, and S. H. Low, "Exact convex relaxation of optimal power flow in radial networks," *IEEE Trans. on Automatic Control*, vol. 60, no. 1, pp. 72–87, Jan. 2015.

[11] W. Shi, N. Li, X. Xie, C. Chu, and R. Gadh, "Optimal residential demand response in distribution networks," *IEEE J. on Selected Areas in Comm.*, vol. 32, no. 7, pp. 1441–1450, Jun. 2014.

[12] E. Dall'Anese, H. Zhu, and G. B. Giannakis, "Distributed optimal power flow for smart microgrids," *IEEE Trans. on Smart Grid*, vol. 4, no. 3, pp. 1464–1475, Sept. 2013.

[13] A. G. Bakirtzis and P. N. Biskas, "A decentralized solution to the DC-OPF of interconnected power systems," *IEEE Trans. on Power Systems*, vol. 18, no. 3, pp. 1007–1013, Aug. 2003.

[14] T. Erseghe, "Distributed optimal power flow using ADMM," *IEEE Trans. on Power Systems*, vol. 29, no. 5, pp. 2370–2380, Sept. 2014.

[15] Q. Peng and S. H. Low, "Distributed algorithm for optimal power flow on a radial network," in *Proc. of IEEE Conf. on Decision and Control*, Dec. 2014, pp. 167–172.

[16] S. Magnusson, P. C. Weeraddana, and C. Fischione, "A distributed approach for the optimal power-flow problem based on ADMM and sequential convex approximations," *IEEE Trans. on Control of Network Systems*, vol. 2, no. 3, pp. 238–253, Sept. 2015.

[17] J. M. Arroyo and F. D. Galiana, "Energy and reserve pricing in security and network-constrained electricity markets," *IEEE Trans. on Power Systems*, vol. 20, no. 2, pp. 634–643, May 2005.

[18] S. Mhanna, A. C. Chapman, and G. Verbič, "A fast distributed algorithm for large-scale demand response aggregation," *IEEE Trans. on Smart Grid*, vol. 7, no. 4, pp. 2094–2107, Jul. 2016.

[19] A. Mohammadi, M. Mehrtash, and A. Kargarian, "Diagonal quadratic approximation for decentralized collaborative TSO+DSO optimal power flow," accepted for publication in *IEEE Trans. on Smart Grid*, Jan. 2018.

[20] M. J. Dolan, E. M. Davidson, I. Kockar, G. W. Ault, and S. D. McArthur, "Distribution power flow management utilizing an online optimal power flow technique," *IEEE Trans. on Power Systems*, vol. 27, no. 2, pp. 790–799, May 2012.

[21] E. Belic, N. Lukac, K. Dezelak, B. Zalik, and G. Stumberger, "GPU-based online optimization of low voltage distribution network operation," accepted for publication in *IEEE Trans. on Smart Grid*, 2017.

[22] R. Hejeejo, J. Qiu, and G. Mirzaeva, "Planning a decentralised and bi-directional market-based management system," *IET Renewable Power Generation*, vol. 11, no. 12, pp. 1555–1564, Nov. 2017.

[23] Z. Wang, B. Chen, J. Wang, and J. kim, "Decentralized energy management system for networked microgrids in grid-connected and islanded modes," *IEEE Trans. on Smart Grid*, vol. 7, no. 2, pp. 1097–1105, Mar. 2016.

[24] L. Gan and S. H. Low, "An online gradient algorithm for optimal power flow on radial networks," *IEEE J. on Selected Areas in Comm.*, vol. 34, no. 3, pp. 625–638, Mar. 2016.

[25] A. Hauswirth, S. Bolognani, G. Hug, and F. Dörfler, "Projected gradient descent on Riemannian manifolds with applications to online power system optimization," in *Proc. of Allerton Conf. on Communications, Control and Computing*, Sept. 2016, pp. 225–232.

[26] S.-J. Kim, G. B. Giannakis, and K. Y. Lee, "Online optimal power flow with renewables," in *Proc. of Asilomar Conf. on Signals, Systems and Computers*, Nov. 2014, pp. 355–360.

[27] S. Bahrami, M.H. Amini, M. Shafie-khah, and J.P.S. Catalao, "A decentralized electricity market scheme enabling demand response deployment," accepted for publication in *IEEE Trans. on Power Systems*, 2017.

[28] D. P. Bertsekas, *Nonlinear Programming*, 2nd ed. Athena scientific, Belmont, Massachusetts, 1999.

[29] W. Deng, M.-J. Lai, Z. Peng, and W. Yin, "Parallel multi-block ADMM with $o(1/k)$ convergence," *Journal of Scientific Computing*, vol. 71, no. 2, pp. 712–736, May 2017.

[30] P. Kundur, N. Balu, and M. Lauby, *Power System Stability and Control.* McGraw-hill New York, 1994.

[31] S. Bahrami, F. Therrien, V. W. S. Wong, and J. Jatskevich, "Semidefinite relaxation of optimal power flow for ac-dc grids," *IEEE Trans. on Power Systems*, vol. 32, no. 1, pp. 289–304, Jan 2017.

[32] D. Bertsimas, E. Litvinov, X. A. Sun, J. Zhao, and T. Zheng, "Adaptive robust optimization for the security constrained unit commitment problem," *IEEE Trans.s on Power Systems*, vol. 28, pp. 52–63, Feb. 2013.

[33] A. Mas-Colell, M. D. Whinston, and J. R. Green, *Microeconomic Theory*, 1st ed. Oxford University Press, 1995.

[34] N. Li, L. Chen, and S. H. Low, "Optimal demand response based on utility maximization in power networks," in *IEEE Power and Energy Society General Meeting*, Jul. 2011, pp. 1–8.

[35] S. Bahrami, V. W. S. Wong, and J. Huang, "An online learning algorithm for demand response in smart grid," accepted for publication in *IEEE Trans. on Smart Grid*, Feb. 2017.

[36] S. Bahrami and V. W. S. Wong, "An autonomous demand response program in smart grid with foresighted users," in *Proc. of IEEE SmartGridComm*, Miami, FL, Nov. 2015, pp. 205–210.

[37] H. Yuan, F. Li, Y. Wei, and J. Zhu, "Novel linearized power flow and linearized OPF models for active distribution networks with application in distribution LMP," *IEEE Trans. on Smart Grid*, vol. 9, no. 1, pp. 438–448, Jan. 2018.

[38] D. P. Bertsekas and J. N. Tsitsiklis, *Parallel and Distributed Computation: Numerical Methods*. Englewood Cliffs, NJ: Prentice Hall, 1989.

[39] G. Chen and M. Teboulle, "A proximal-based decomposition method for convex minimization problems," *Mathematical Programming*, vol. 64, no. 1, pp. 81–101, Mar. 1994.

[40] IEEE Test Feeders (accessed: Jan. 2017). [Online]. Available: https://ewh.ieee.org/soc/pes/dsacom/testfeeders/

[41] Independent Electricity System Operator (IESO) (accessed: Mar. 2017). [Online]. Available: http://www.ieso.ca

[42] Torontohydro website (accessed: Feb. 2017). [Online]. Available: http://www.torontohydro.com/sites/electricsystemresidential/yourbilloverview/Pages/ApplianceChart.aspx

[43] P. Samadi, S. Bahrami, V. Wong, and R. Schober, "Power dispatch and load control with generation uncertainty," in *Proc. of IEEE Global Conf. on Signal and Information Processing (GlobalSIP)*, Dec. 2015, pp. 1126–1130.

[44] S. Bahrami and V. Wong, "Security-constrained unit commitment for ac-dc grids with generation and load uncertainty," accepted for publication in *IEEE Trans. on Power Systems*, 2017.

1949-3029 (c) 2018 IEEE. Personal use is permitted, but republication/redistribution requires IEEE permission. See http://www.ieee.org/publications_standards/publications/rights/index.html for more information.

This article has been accepted for publication in a future issue of this journal, but has not been fully edited. Content may change prior to final publication. Citation information: DOI 10.1109/TSTE.2018.2815502, IEEE Transactions on Sustainable Energy

Shahab Bahrami (S'12, M'18) received the B.Sc. and M.A.Sc. degrees both from Sharif University of Technology, Tehran, Iran, in 2010 and 2012, respectively. He received the Ph.D. degree from the University of British Columbia (UBC), Vancouver, BC, Canada in 2017. Dr. Bahrami continued to work as a post-doctoral research fellow at UBC until Jan. 2018. Dr. Bahrami has received various prestigious scholarships at UBC, including the distinguished and highly competitive UBC's Four Year Fellowship (2013-2017) as well as the Graduate Support Initiative Award from the Faculty of Applied Science at UBC (2014-2017). Dr. Bahrami also received a Best Paper Award at the *IEEE Pacific Rim Conf. on Communications, Computers and Signal Processing (PACRIM 2015)*. His research interests include optimal power flow analysis, game theory, and demand side management, with applications to smart grid.

M. Hadi Amini (S'11, GSM'13), is currently a Ph.D. Candidate with the Department of Electrical and Computer Engineering, Carnegie Mellon University, Pittsburgh, PA, where he received the M.Sc. degree in Electrical and Computer Engineering in 2015. Prior to that, he received the B.Sc. degree from the Sharif University of Technology, Tehran, Iran, in 2011, and the M.Sc. degree from Tarbiat Modares University, Tehran, in 2013, both in Electrical Engineering. He serves as the lead-Editor for the book entitled "*Sustainable Interdependent Networks: From Theory to Application*". He is the recipient of the best paper award of "*Journal of Modern Power Systems and Clean Energy*" in 2016, best reviewer award of "*IEEE Trans. on Smart Grid*" from the IEEE Power & Energy Society in 2017, outstanding reviewer award of "*IEEE Trans. on Sustainable Energy*" in 2017, and the dean's honorary award from the president of Sharif University of Technology in 2007. Hadi is a member of IEEE-Eta Kappa Nu (IEEE-HKN) Sigma Chapter, the honor society of IEEE. His research interests include distributed algorithms, interdependent networks, electric vehicles, demand response, and state estimation. (Homepage: www.HadiAmini.com)

Miadreza Shafie-khah (S'08, M'13, SM'17) received the M.Sc. and Ph.D. degrees in electrical engineering from Tarbiat Modares University, Tehran, Iran, in 2008 and 2012, respectively. He received his first postdoc from the University of Beira Interior (UBI), Covilhã, Portugal in 2015, while working on the 5.2-million-euro FP7 project SiNGULAR ("Smart and Sustainable Insular Electricity Grids Under Large Scale Renewable Integration"). He received his second postdoc from the University of Salerno, Salerno, Italy in 2016. He is currently a Visiting Scientist (position only awarded to PhD holders who have scientific curricula of high merit, equivalent to Assistant Professor) and Senior Researcher at CMAST/UBI, where he has a major role of coordinating a WP in the 2.1-million-euro national project ESGRIDS ("Enhancing Smart GRIDS for Sustainability"), while co-supervising 4 PhD students and 2 postdoc fellows. He was considered one of the Outstanding Reviewers of *IEEE TSTE*, in 2014, and one of the *IEEE TSG* Best Reviewers in 2016. His research interests include power market monitoring and simulation, power system optimization, demand response, electric vehicles, price forecasting and smart grids.

João P. S. Catalão (M'04, SM'12) João P. S. Catalão (M'04-SM'12) received the M.Sc. degree from the Instituto Superior Técnico (IST), Lisbon, Portugal, in 2003, and the Ph.D. degree and Habilitation for Full Professor (("Agregação")) from the University of Beira Interior (UBI), Covilha, Portugal, in 2007 and 2013, respectively.

Currently, he is a Professor at the Faculty of Engineering of the University of Porto (FEUP), Porto, Portugal, and Researcher at INESC TEC, INESC-ID/IST-UL, and C-MAST/UBI. He was the Primary Coordinator of the EU-funded FP7 project SiNGULAR ("Smart and Sustainable Insular Electricity Grids Under Large-Scale Renewable Integration"), a 5.2-million-euro project involving 11 industry partners. He has authored or coauthored more than 620 publications, including 220 journal papers (more than 65 IEEE Transactions/Journal papers), 350 conference proceedings papers, 2 books, 34 book chapters, and 14 technical reports, with an h-index of 37, an i10-index of 139, and over 5675 citations (according to Google Scholar), having supervised more than 50 post-docs, Ph.D. and M.Sc. students. He is the Editor of the books entitled *Electric Power Systems: Advanced Forecasting Techniques and Optimal Generation Scheduling* and *Smart and Sustainable Power Systems: Operations, Planning and Economics of Insular Electricity Grids* (Boca Raton, FL, USA: CRC Press, 2012 and 2015, respectively). His research interests include power system operations and planning, hydro and thermal scheduling, wind and price forecasting, distributed renewable generation, demand response and smart grids.

Prof. Catalão is an Editor of the *IEEE Trans. on Smart Grid*, an Editor of the *IEEE Trans. on Power Systems*, and an Associate Editor of the *IET Renewable Power Generation*. From 2011 till 2018 (seven years) he was an Editor of the *IEEE Trans. on Sustainable Energy*. He was the Guest Editor-in-Chief for the Special Section on "Real-Time Demand Response" of the *IEEE Trans. on Smart Grid*, published in December 2012, and the Guest Editor-in-Chief for the Special Section on "Reserve and Flexibility for Handling Variability and Uncertainty of Renewable Generation" of the *IEEE Trans. on Sustainable Energy*, published in April 2016. Since May 2017, he is the Corresponding Guest Editor for the Special Section on "Industrial and Commercial Demand Response" of the *IEEE Trans. on Industrial Informatics*. He was the recipient of the 2011 Scientific Merit Award UBI-FE/Santander Universities, the 2012 Scientific Award UTL/Santander Totta, the 2016 FEUP Diploma of Scientific Recognition, and the Best INESC-ID Researcher 2017 Award, in addition to an Honorable Mention in the 2017 Scientific Awards ULisboa/Santander Universities. Moreover, he has won 4 Best Paper Awards at IEEE Conferences.

1949-3029 (c) 2018 IEEE. Personal use is permitted, but republication/redistribution requires IEEE permission. See http://www.ieee.org/publications_standards/publications/rights/index.html for more information.